

CHEMOSTRATIGRAPHY OF THE MISSISSIPPIAN- AGE
BARNETT FORMATION, FORT WORTH BASIN,
WISE COUNTY, TEXAS
USA

by

CHIZOBA CHARITY NSIANYA

Presented to the Faculty of the Graduate School of
The University of Texas at Arlington in Partial Fulfillment
of the Requirements
for the Degree of

MASTER OF SCIENCE IN GEOLOGY
THE UNIVERSITY OF TEXAS AT ARLINGTON
MAY 2013

Copyright © by Student Chizoba Nsianya 2013

All Rights Reserved



Acknowledgements

I would like to thank Dr. Rowe for his support, patience and insights throughout the development of this project. I also give special thanks to Dr. Wickham for his advice and for helping me follow my path at UTA. I would like to thank the staff and administrators of the Department of Earth's and Environmental sciences for all their help during my years in graduate school. I also thank Dr. Nestell for being one of my thesis committee members.

I am so grateful to Texas Bureau of Economic Geology, Jacksons School of Geoscience (UT Austin), for providing access to the core, and for their help throughout this project. I want to thank Rene for his assistance and discussions on geochemistry. I express my gratitude to the staff of Greyfox Energy LLP, for their support and help whenever I needed it; I am blessed to be part of you.

I cannot thank my family enough especially my mum for being there to take care of the kids at odd times. Above all, I would like to thank my husband for putting up with a busy and absent wife, for taking care of the kids, for being everything I could ask for in a partner. This thesis would have been impossible without your help and encouragements

April 16, 2013

Abstract

CHEMOSTRATIGRAPHY OF THE MISSISSIPPIAN- AGE
BARNETT FORMATION, FORT WORTH BASIN,
WISE COUNTY, TEXAS
USA

Chizoba Nsianya, M.S

The University of Texas at Arlington, 2013

Supervising Professor: Harold Rowe

The Mississippian- age Barnett Formation is a shale-gas system dominated by fine grained clay- to silt –size particles deposited in the Fort Worth Basin, a peripheral foreland basin that formed during the late Paleozoic as a result of continental collision between Laurasia and Gondwana. A detailed assessment of the chemostratigraphy and depositional environment of the Barnett Formation in the northern end of Fort Worth Basin, Texas will be studied using a variety of geochemical methods. One drill core located in the south-eastern part of Wise County (Texas, USA) was scanned at high resolution (~ 2 inch interval) using a hand- held X-ray fluorescence (ED-XRF) spectrometer in order to provide a quantitative analysis of its major (e.g. Si, Ca ,Al) and trace (e.g. MO, U, V) element geochemistry. Furthermore, total organic carbon (TOC), total inorganic

carbon (TIC) and total nitrogen (TN) data were collected at one-foot sample spacing. Major element geochemistry (Si/Al) suggests a silica rich mudstone; however relative proportions of % silica (SiO_2) and Zircon (Zr) suggest that most of this excess silica in the Barnett Formation is biogenic in origin. Trace element relationships reveal that the Barnett Formation in the northern Fort Worth Basin was deposited under anoxic/euxinic conditions with relatively high total organic carbon concentration ranging from 2.0 to approximately 8 %. The organic matter provenance was determined to be primarily of marine origin. Changes in the stratigraphy using $\text{EF}_{\text{Fe/Al}}$ together with DOP_T also confirm that the Barnett Formation (lower interval) contains abundant iron relative to normal gray shale.

Table of Contents

Acknowledgements.....	iii
Abstract.....	iv
List of Illustrations.....	ix
List of Tables.....	xi
Chapter 1 Introduction.....	1
1.1 Project Aspiration.....	1
1.1.1 Mudrock research.....	1
1.1.2 Previous Geochemical studies of the Barnett Formation.....	2
1.2 Geologic Setting.....	3
1.2.1 Geographic Setting and Structure of Fort Worth Basin (FWB).....	3
1.2.2 Tectonics and Structural Geology of FWB.....	5
1.2.3 Generalized stratigraphy of FWB.....	8
1.2.4 Barnett Formation.....	10
1.3 Research Objectives.....	13
Chapter 2 Analytical Methods and Data Acquisition.....	14
2.1 Core Information	14

2.2 Energy Dispersive X-ray Fluorescence (ED-XRF)	
Analysis.....	16
2.2.1 Mudstone Calibration of ED-XRF.....	17
2.3 Additional Geochemical Analysis	
(TOC, TIC, TN, LECO-S etc.).....	19
Chapter 3 Results.....	20
3.1 Core Chemostratigraphy.....	21
3.1.1 Major elements/Terrigenous input.....	21
3.1.2 Non-XRF data, Trace metals and Depositional	
Environment.....	22
3.1.3 Integrated data (Ternary Plots, organic matter	
composition and provenance).....	24
3.1.4 Tables.....	43
Chapter 4 Discussion.....	47
4.1 Major elements/Terrigenous input.....	47
4.2 Trace elements and non-XRF data (TOC, TIC etc.).....	50
4.2.1 Basinal restriction.....	52
4.2.2 Sulfur-Iron-TOC Relationship.....	52
4.2.3 Degree of Pyritization (DOP).....	54
4.2.3 Organic matter composition and provenance.....	55
Chapter 5 Conclusions.....	59

References.....	61
Biographical Information.....	69

Lists of Illustrations

Figure 1.1 Map of Fort Worth Basin (FWB).....	4
Figure 1.2 Regional paleogeography of the southern mid-continent.....	7
Figure 1.3 Generalized stratigraphy of FWB.....	9
Figure 1.4 Schematic cross-section of FWB.....	11
Figure 1.5 Isopach map of Barnett Formation.....	12
Figure 2.1 Map of Texas with core location.....	14
Figure 3.1 Chemostratigraphic plots of major elements.....	25
Figure 3.2 Cross-plots of Ti and K against Al.....	26
Figure 3.3 Cross-plot of Si versus Al.....	27
Figure 3.4 Cross-plot of Fe versus Al.....	28
Figure 3.5 Cross-plot of Mg against Al.....	29
Figure 3.6 Cross-plot of S against Fe.....	30
Figure 3.7 Cross-plot of SiO ₂ against Zr.....	31
Figure 3.8 Cross-plot of Ca versus TIC.....	32
Figure 3.9 Chemostratigraphic plot of anoxic indicators.....	33
Figure 3.10 Cross-plot of silicon-excess against enrichment factor Mo over Al.....	34
Figure 3.11 Cross-plots of geochemical data with depth.....	35
Figure 3.12 Cross-plot of LECO sulfur versus TOC.....	36
Figure 3.13 Chemostratigraphic plots of non-XRF data.....	37

Figure 3.14 Calcite-clay-quartz ternary plot.....	38
Figure 3.15 Fe-S-TOC ternary diagram.....	39
Figure 3.16 Identifier of the Organic matter provenance.....	40
Figure 3.17 Organic matter source using $\delta^{13}\text{C}$ and $\delta^{15}\text{N}$	41
Figure 3.18 Cross-plots of trace elements versus TOC.....	42

Lists of Tables

Table 2.1 General core information.....	15
Table 2.2 Instrumentation and settings used for Mudstone calibration.....	18
Table 2.3 Types and number of samples analyzed.....	19
Table 3.1 Average major elemental values for Blakely # 1.....	44
Table 3.2 Average trace elemental values for Blakely # 1.....	45
Table 3.3 Average values for TOC, TIC, TN, $\delta^{13}\text{C}$ and $\delta^{15}\text{N}$	46

Chapter 1

Introduction

1.1 Project Aspiration

1.1.1 Mudrock research

Over the years the study of mud and mudstones has lagged far behind that of other lithologies, a circumstance that is in part due to their fine-grained nature. Most of the sedimentary particles that compose mudrock are less than 0.0625 mm, and are too small to be studied readily in the field due to their diminutive sizes which make them susceptible to weathering on outcrops. Yet, within petroleum systems mudrocks are important sources of hydrocarbon and typically are also important as hydrocarbon seals.

According to Alplin et al (1999), these mudrock systems make up fifty percent of the sedimentary rocks in the geologic record and are by far the dominant sedimentary rock. Additionally, the geologic studies of mudrocks are also vital because mudrocks contain a variety of trace elements which may provide good record of their paleoceanography and depositional environments (Algeo and Rowe, 2011). Mudrocks are also of great academic interest, because major mineral deposits like lead, zinc, manganese, barite and copper occur in them. Metamorphosed shales are also hosts for emeralds and gold (Potter et al.,

2004). The Barnett Formation is a succession of organic-rich black shale with great interest to mudrock researchers, because of its excellent petroleum system element (its own source, reservoir, seal and stratigraphic trap). Outcrop observation has yielded relatively few data for interpreting the origin and factors governing the formation of the Barnett Formation (Pollastro et al.; 2003). Recent studies (Henry, 1982; Curtis, 2002; Pollastro et al.; 2003) have demonstrated that mudrocks are extremely complex and diverse, and complete understandings of them are still in development. However, a growing body of chemical data both on organic and inorganic constituents of black shale will widen the scope of inferences that can be drawn on the genesis of such rocks (Tourtelot, 1979). Formation of black shale throughout the earth's history in all parts of the world suggests that geologic processes not geologic settings control the factors that lead to its accumulation. The primary constituent of black shale is mud or clay-size particles; they also contain calcium carbonate (CaCO_3) and other major constituent such as biogenic silica (SiO_2).

1.1.2 Previous Geochemical studies of the Barnett Formation

Several geochemical studies have been carried out on the Barnett Formation. Most of these studies have been conducted primarily on the organic, petroleum and petrophysics attributes of the Barnett Formation. Kane, (2006) and Loucks et al., (2009), gave a detailed description on the petrophysical

characterization of the Barnett Formation. Javie et al., (2006) published an excellent work on the organic and gas generation potential of the Barnett Formation. Montgomery, (2004 and 2005) published an extensive summary of the Barnett Formation in the Fort Worth Basin. However, there are few published works on the inorganic geochemistry of the Barnett Formation. To solve stratigraphic uncertainties that affect well-to-well correlation and facies analysis, it is vital to analyze the elemental composition of these rocks.

1.2 Geologic Setting

1.2.1 Geographic Setting and Structure of Fort Worth Basin

The Fort Worth Basin is a peripheral foreland basin (Paleozoic in age) primarily located in north central Texas and south western Oklahoma (Fig 1.1). The Province boundary of Fort Worth Basin generally follows the Ouachita structural front to the east and southeast, the Texas-Oklahoma State line (the Red River Arch) to the north, the Llano Uplift to the south and the Bend Arch to the west (Fig1.1). The asymmetrical, wedge-shaped Fort Worth Basin is approximately 200 miles long and ranges in width from more than 100 miles on the northern end to less than 10 miles on its southern end where it terminates at the Llano Uplift (Walper, 1982).

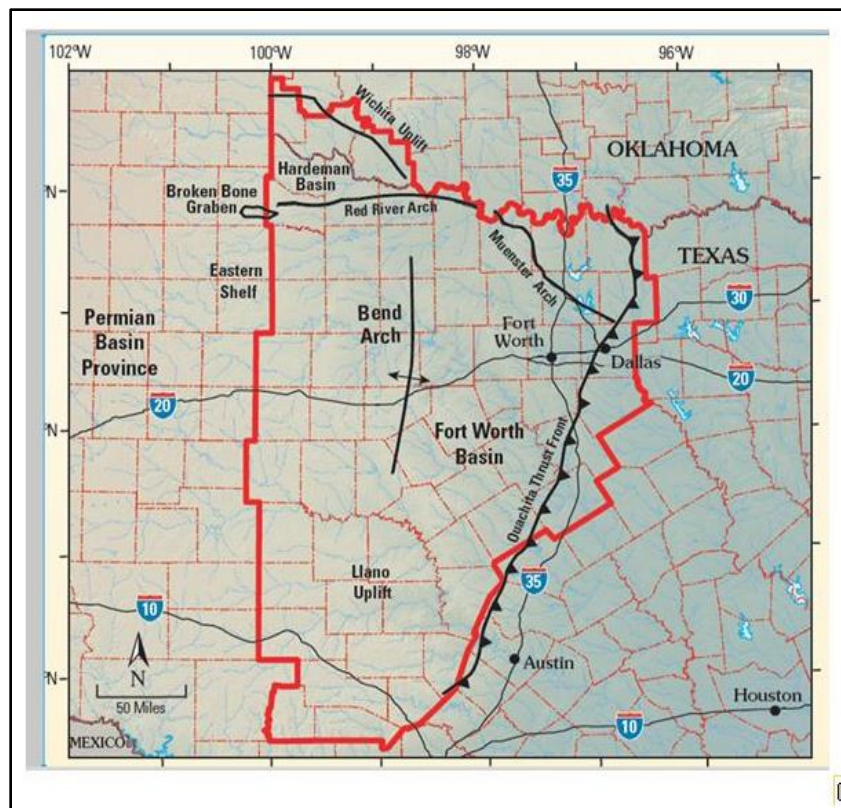


Figure 1.1 Map of Fort Worth Basin showing its major structural features (Pollastro et al., 2007)

1.2.2 Tectonics and Structural Geology of Forth Worth Basin

The Fort Worth Basin is one of the basins of the Ouachita structural belt which formed due to continental collision between the Laurasia and Gondwana paleocontinents in late Paleozoic (Thomas, 2002). The basin's origin and development has been discussed from many points of view (Turner, 1958; Flawn et al., 1961, Hodgen and Martin, 1974) and the general consensus reached is that the basin is a preserved remnant of the Ouachita geosynclines. Although a number of papers have dealt with the collision of North and South America and the formation of the Ouachita Fold belt (Walper and Rowett, 1972; Ingersoll and Dickinson, 1975; Walper, 1977), few have dealt with the evolution of the Fort Worth Basin within a plate tectonic framework. Although the Fort Worth Basin emerged as a foreland basin; its geodynamic history starts from passive plate margin to continental orogen. Several linked processes such as volcanism, metamorphism and sedimentation affected the various stages of the basin's evolution. The southern margin of Laurasia became a retreating and subsiding plate margin dominated by carbonate deposition from Cambrian to Ordovician time after the rifting of Laurasia from Gondwana in the late Precambrian (Walper,1982). A reversal in subduction polarity during Silurian and Devonian time caused Laurasia to become the subducting plate (Jurdy et al., 1995). The reorientation in plate motion caused the volcanic arc at the outer edge of the

marginal basin to become the consuming plate as its lithosphere was subducted (Walper, 1982). The subducted marginal basin crust was consumed and the sedimentary strata which filled the basin from the down-going plate were also scraped and piled into a growing subduction complex which eventually overthrust the subducting margin of Laurasia (Walper, 1982). The subduction complex became the base of the Ouachita facies rocks, which grew into the Ouachita foldbelt (Walper, 1982). The Fort Worth Basin formed in response to flexural loading due the advancing Ouachita thrust belt (Flippen, 1982). The Fort Worth Basin subsided substantially during early to late Pennsylvanian time as a result of the advancing Ouachita thrust. Subsidence of the basin was asymmetrical to the northern end and was likely related to the flexural loading of the continental crust (Kier et al., 1979). Several faults that cut basement and lower Paleozoic rocks in the southern part of the basin are identified at the Ordovician Ellenburger group stratigraphic level. These faults and associated structures formed during development of the Llano uplift and Fort Worth Basin. These faults run northeast-southwest through Palo Pinto, Parker, Wise and Denton counties to join with the Newark East fault system (Thompson, 1988).

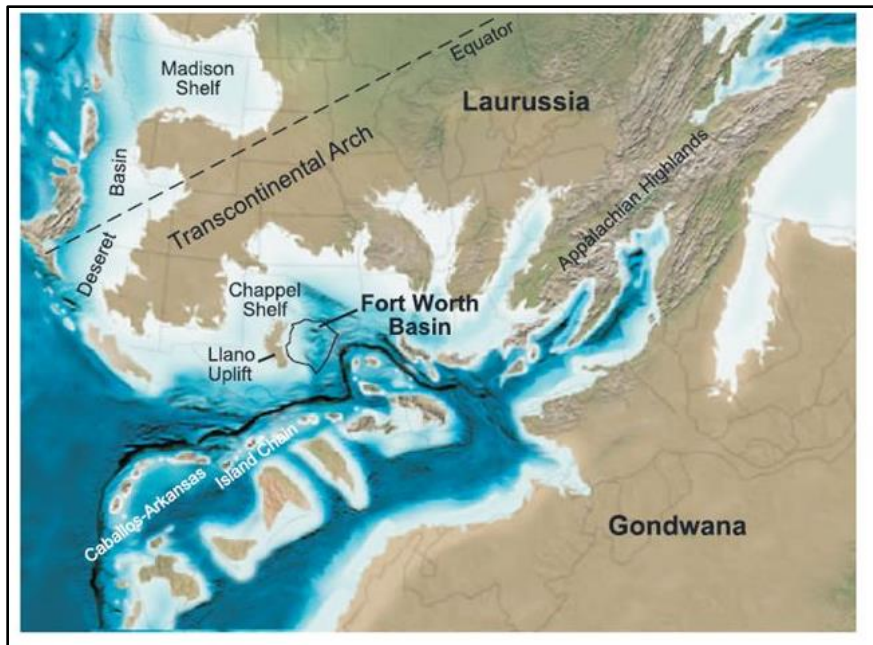


Figure 1.2 Regional paleogeography of the southern mid-continent region during the late Mississippian (325 Ma) showing the approximate position of the Fort Worth Basin. Plate reconstruction by Blakey (2005).

1.2.3 Generalized Stratigraphy of Fort Worth basin

Figure 1.3 shows the general stratigraphic column of the Fort Worth Basin. The sedimentary section of the Fort Worth Basin is underlain by Precambrian diorite and granite. Granite conglomerate, sandstones, and shale make up the Cambrian rocks and are overlain by marine carbonate rocks and shale (Flippen, 1982).

Based on the depositional history interpreted by Montgomery et al., (2005), the Paleozoic section of the basin is divided into 3 intervals: (1) Cambrian–Upper Ordovician platform strata (Riley–Wilberns, Ellenburger, Viola, and Simpson), which were deposited on a stable cratonic shelf ; (2) middle–upper Mississippian strata (Chappel Formation, Barnett Formation, and lower Marble Falls Formation), deposited during the early phases of subsidence related to tectonism along the Oklahoma aulacogen; and (3) Pennsylvanian Strata (upper Marble Falls Formation, Atoka, etc.), representing the main phase of subsidence related to the advancing Ouachita thrust belt. The Ellenburger group is mostly limestone and dolomites and has karsting due to dissolution in some part of Fort Worth Basin. The Chappel and Barnett Formation lie unconformably (in some part of the basin) upon the Ellenburger and Viola Formations. The Chappel Formation is a crinoidal limestone (Montgomery et al, 2005); while the Barnett Formation is a thick, organic-rich black shale and is considered as the source rock

for most of the Paleozoic reservoirs in Fort Worth Basin. Overlying the Barnett Formation are the Marble Falls carbonate bank and the Atoka clastic rocks which were deposited the early and middle Pennsylvanian respectively.

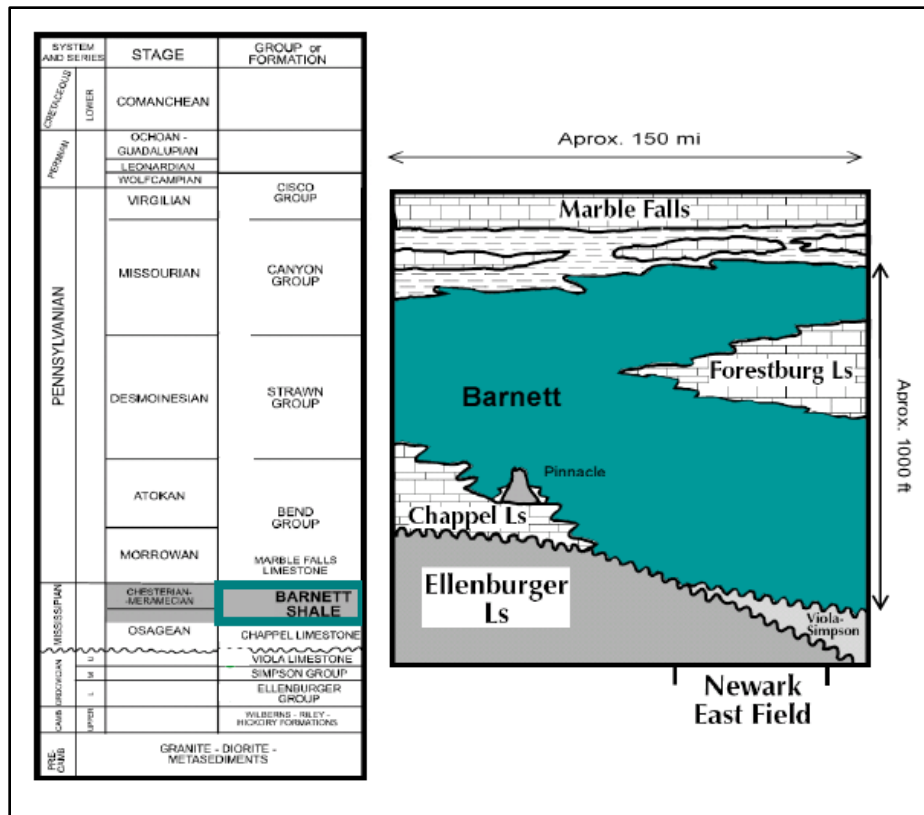


Figure 1.3 Generalized stratigraphy of the Fort Worth Basin (taken from Singh, 2008. Modified from Montgomery et al, 2005)

1.2.4 Barnett Formation

The Mississippian-age Barnett Formation has been described as black shale with petroliferous characteristics; the unit was named after the Barnett springs close to San Saba County, where it is exposed (Plummer and Moore, 1921). The uplifting of the Ouachita orogeny during the Mississippian period led to the reactivation of the Muenster and Red River Arch (Walper, 1982). All these structural features affected the deposition of the Barnett Formation. On the basis of sediment thickness, published cross sections (Fig 1.4) and isopach map (Fig 1.5) show that the unit has its greatest thickness (up to 1000 feet) towards the northeast part of Fort Worth Basin and thins progressively towards the south and southwest (Loucks and Ruppel, 2006). In the study area, the Barnett Formation is divided into the upper and lower sections due to the presence of the Forestburg limestone, an interval of carbonate-rich sediments (Fig 1.2.3.1). Where the Forestburg limestone is absent, the Barnett Formation is considered a single and undifferentiated unit. The Barnett Formation is absent over the Muenster Arch, and is not considered a true shale at the core location because of lack of fissility (Rowe et al, 2008).

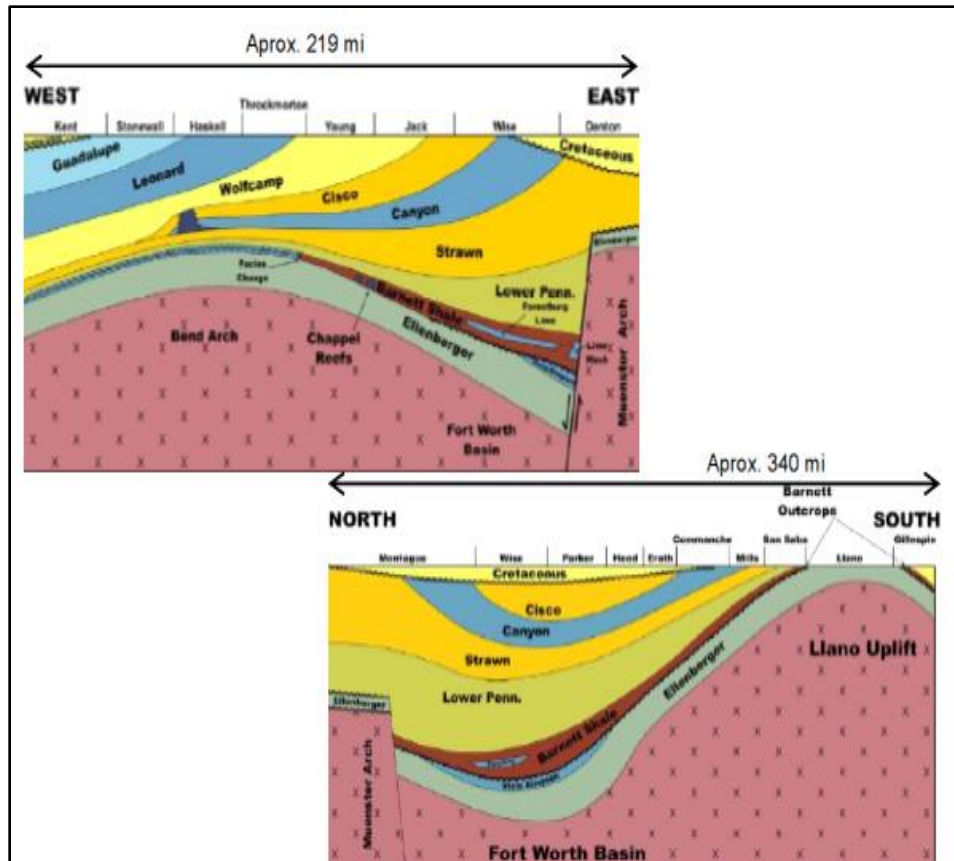


Figure 1.4 Schematic cross section of Fort Worth Basin. The thickness of the Barnett Formation in Wise County is approximately 550 ft. (Hayden and Pursell, 2005).

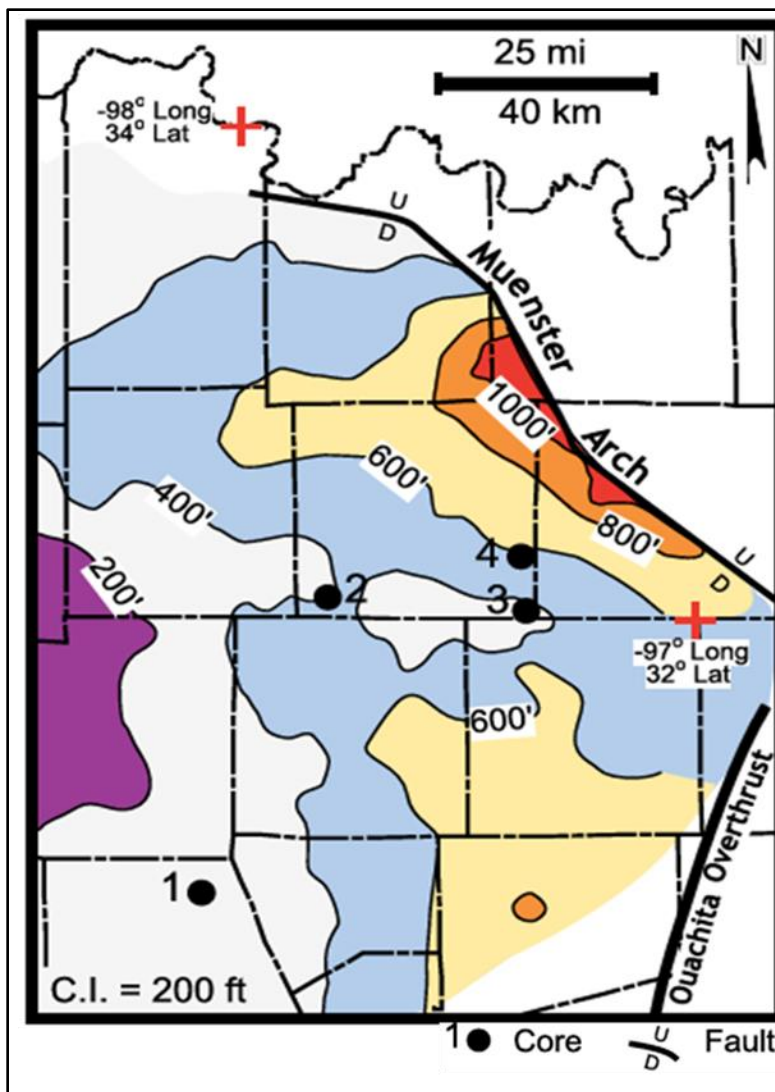


Figure 1.5 Isopach map of Barnett Formation based on wire-line-log correlation (taken from Loucks and Ruppel, 2006)

1.3 Research Objective

The geochemistry of sedimentary rocks is the result of their provenance, depositional settings, and diagenetic history (Andrew et al, 1996). Such analysis of mudrock is necessary to be able to observe subtle differences during deposition (e. g., Rowe et al., 2008). Chemostratigraphy or chemical stratigraphy, involves the characterization and correlation of strata using major and trace element geochemistry and provides diverse applications for investigating the rock record, such as reconstructing paleoenvironments, determining the tectonic setting of sedimentary basins, indirect dating, and establishing regional or global correlations. Chemostratigraphy is becoming an integral component for many investigations of the ancient sedimentary record. Given the little published work on sedimentology, lithofacies and depositional setting of the Barnett Formation (Loucks and Ruppel, 2006), the purpose of this research is to better understand the depositional environment of the Barnett Formation by relating variations in the rock chemistry to changes in the environment in which it was deposited. Chemostratigraphic data of major elements (e.g. Al, Si, and Ca) is used to identify changes in mineralogy, differentiate stratigraphic changes in lithology and can thus be very useful in correlation. Variation in the trace element concentration reflects difference in source and depositional environment.

Chapter 2

Analytical Methods and Data Acquisition

2.1 Core Information

One drill core collected from southeastern part of Wise County, Texas in the Northern end of Fort Worth Basin was analyzed. The core was drilled by Texas United Oil and Gas Incorporated and housed at the Core Research Center of the Bureau of Economic Geology in Austin, Texas. The general information of the analyzed core is presented in Table 2.1 while the core location is shown in figure 2.1.

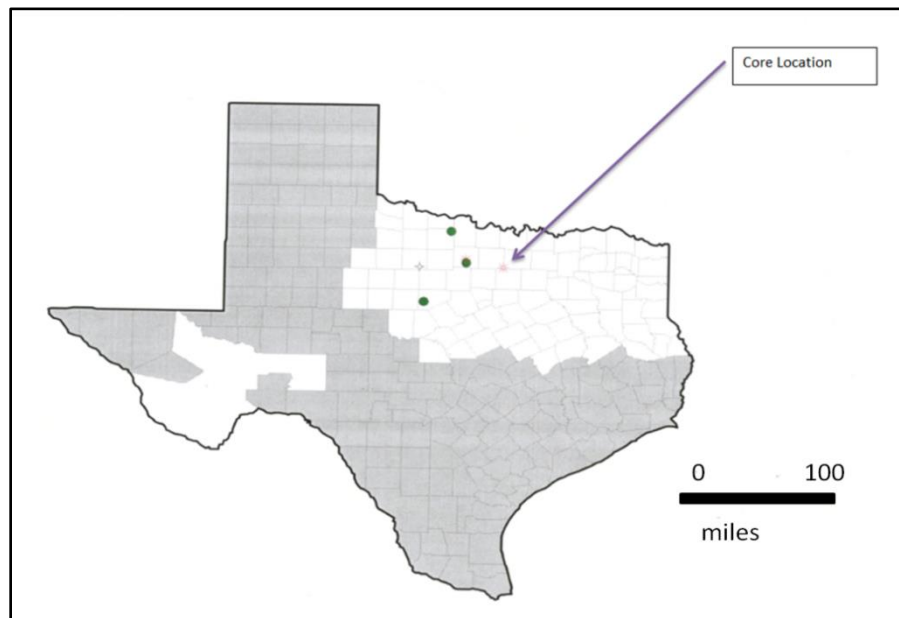


Figure 2.1 Map of Texas, arrow showing core/well location (source: IHS PI Dwight CD 2012. Texas and Oklahoma well data)

Table 2.1 General core information

OPERATOR	COUNTY (TX)	LEASE NAME	WELL #	LOCATION (lat/long)	GEOLOGIC PROVINCE	API #	XRF UNIT UTILIZED	INTERVAL ANALYZED
TEXAS UNITED O&G INC	WISE	BLAKELY	1	33.0056183 / -97.4003555	FORT WORTH SYNCLINE	42497330410000	BEG XRF	7100-7225

2.2 Energy Dispersive X-ray Fluorescence (ED-XRF) Analysis

Core samples were analyzed for major and trace element geochemistry using a Bruker Tracer III-V handheld ED-XRF spectrometer at approximately 2 inches interval. The instrument has a great advantage because of its ability to analyze samples without destructive sample preparation procedures. Each core sample was slabbed and made flat to ensure accurate measurement sensitivity of the instrument. The flat surface of each sample was placed on the nose of the instrument above the 3 X 4 mm elliptical beam window and stabilized using a platform that surrounded the nose of the instrument. With a low energy, vacuum-pumped instrument setting at 15 Kv, each sample was analyzed for major element concentration for 60 seconds. Trace elemental analysis of each sample was also carried out using a filtered high energy instrument setting (40Kv). The filter was inserted into the instrument and helps to prevent low-energy x-rays from reaching the detector. Each sample was analyzed for trace elemental concentration for 120 seconds. Both the major and trace element analysis of the samples were carried out at the core laboratory of the Bureau of Economic Geology in Austin, Texas.

2.2.1 Mudstone calibration of ED-XRF

To define Chemostratigraphic changes in real time, it is vital that the handheld ED-XRF is calibrated while undertaking analysis of mudstone (Rowe and Hughes, 2010). The energy spectra from core samples were calibrated using a suite of reference materials (Rowe and Hughes, 2010) in order to quantify down-core changes in geochemistry. The suite of reference materials used for the calibration of major element (low- energy) and trace element (high-energy) measurements are listed below:

- ❖ Five international shale standards.
- ❖ Seven from the Devonian-Mississippian Ohio shale.
- ❖ Twenty from the Pennsylvanian Smithwick Formation, Fort Worth Basin.
- ❖ Twenty eight from the Devonian – Mississippian Woodford Formation, Permian Basin.
- ❖ Fifteen from the Cretaceous Eagle Ford Formation, Gulf Coast, Texas.
- ❖ Sixteen from the Mississippian Barnett Formation, Fort Worth Basin.

Each of the ninety reference materials was pressed in a Carver press to forty tons with a forty millimeter die using a boric acid backing (Rowe and Hughes, 2010) Each reference material was pulverized to approximately 8 grams of 200 mesh powder using a TM engineering pulverizer with trace metal grade stainless steel pulverizing cups and pucks (Rowe and Hughes, 2010).

The instrumentation and setting for the major and trace elemental calibration is shown in Table 2.2. The low -energy calibration quantifies the following elements: Mg, Al, Si, P, S, K, Ca, Ba, Ti, V, Cr, Mn, and Fe; while the high-energy calibration quantifies the following: Ni, Cu, Zn, Th, Rb, U, Sr, Y, Zr, Nb, and Mo. The standard pellets were analyzed (3 times) on its face under both low and high-energy settings for six minutes. All 270 raw x-ray spectra (90 references x 3 analyses) were loaded into Bruker’s CalProcess software along with the accepted elemental concentrations for all standards. Slope and background inter-element correction was performed for each element. Rowe and Hughes, 2010 illustrates a more detailed evaluation of the calibration process.

Table 2.2 Instrumentation and settings used for mudstone calibration

Instrument	Low –energy setting	High-energy setting
Bruker Tracer III/V ED-X	15 kV, 42 μ A, no filter	40kV, 28 μ A, Cu-Ti-Al filter

2.3 Additional Geochemical Analysis (TOC, TIC, TN, LECO-S, etc.)

Samples were collected at one-foot sample spacing and analyzed for sulfur, total organic carbon (TOC), total inorganic carbon (TIC) and total nitrogen (TN). TIC analysis was performed using a UIC, Inc. coulometer (Eagleman et al, 1985) with standard unknown standard deviations of <0.5%. Total organic carbon (TOC), total nitrogen (TN), stable isotopic compositions of TOC ($\delta^{13}\text{C}$) and TN ($\delta^{15}\text{N}$) analysis were performed on powdered samples. Please refer to Rowe et al, 2008 for a detailed description on data collection regarding TOC, TIC, TN, sulfur (LECO-S), TOC ($\delta^{13}\text{C}$) and TN ($\delta^{15}\text{N}$) isotopic compositions.

Table 2.3 Types and number of samples analyzed

CORE NAME	XRF	TOTAL INORGANIC CARBON (TIC)	TOTAL ORGANIC CARBON (TOC)	TOTAL PERCENTAGE NITROGEN (TN)	CARBON ISOTOPES ($\delta^{13}\text{C}$)	NITROGEN ISOTOPES ($\delta^{15}\text{N}$)	SULFUR (LECO-S)
BLAKELY # 1	696	128	128	128	128	128	128

Chapter 3

Results

Several cross-plots were generated using geochemical data obtained from X-ray fluorescence spectrometry and other geochemical analysis as described in chapter 2. These plots are expressed in weight percent (e.g. %Al), parts per million (e.g. Mo), degree of pyritization (DOP), whole number ratio (Fe/Ti) or as enrichment factors (EF) which is expressed by the following equation:

$$EF = (\text{element in ppm/Al in ppm})_{\text{sample}} / (\text{element in ppm/Al in ppm})_{\text{standard}}$$

The degree of pyritization (DOP) are approximated using DOP_T and is defined as pyritic iron/total iron (Raiswell and Berner, 1986).

Two different sets of data are presented for X-ray fluorescence spectrometry (XRF) and non- XRF data using the Blakely # 1 core (table 2.3). The silica excess parameter % Si-excess is calculated as the absolute %Si difference between the measured % Si of a sample and the %Si versus %Al regression line for the lower Barnett argillaceous mudstone (Rowe et al,2008). All enrichment factors are calculated based on values for average marine gray shale (Wedepohl, 1971, 1991)

3.1 Core Chemostratigraphy

3.1.1 Major elements /Terrigenous input

Inter-elemental relationships are observed using cross-plots of major elements. Variations of selected elements are also observed when plotted against depth and is used to determine changes in bulk mineralogy. Figure 3.1 is a plot of major elements (Si, Al, Ca and P) with depth showing Chemostratigraphic identification between the upper and lower Barnett Formation and the intervening calcareous Forestburg limestone. Aluminum is traditionally linked to clay minerals (e.g. illite), each element in clay and non-clay mineral phases are identified using cross-plots of major elements versus aluminum. Terrigenous inputs are also recognized utilizing cross-plots of Al against Ti, K and Si (can be associated with biogenic quartz). Cross-plots of Ti and K against Al in Figure 3.2 show a strong correlation between these elements and Al. The dominance of clay in the upper and lower Barnett Formation is also shown in Figure 3.2 by higher concentration of Al. Silicon also exhibit a good relationship with Al in Figure 3.3 however, many data points to the left of the graph indicate Si enrichment relative to Al. Figure 3.4 is a cross-plot of Fe versus Al, the positive correlation observed indicate the association of iron in the clay minerals, also notice the enrichment in iron concentration in some of the lower Barnett samples.

Figure 3.5 is a cross-plot of Mg (a proxy for dolomitic input) versus Al, notice that the Forestburg samples are relatively rich in Mg when compared to the Barnett samples, also notice the increase in Mg concentration in some of the lower Barnett samples. Figure 3.5 also depicts the higher concentration of Al over Mg in most of the upper and lower Barnett samples. Figure 3.6 cross is a plot of Fe versus S showing a fairly good correlation between the two elements. However, some samples show Fe enrichment relative to S. Zr is associated with heavy mineral Zircon; Figure 3.7 shows increase in SiO₂ concentration over Zr.

3.1.2 Non-XRF data, Trace Metals and Depositional environment

Figure 3.8 is a cross-plot of total inorganic carbon (TIC) versus calcium. Calcium shows a very strong linear trend with TIC, notice the high concentration of TIC with Ca increase within the Forestburg samples. Anoxic indicators (Mo, V, and U) and redox sensitive element Zn are plotted against depth in Figure 3.9; Mo shows a moderate enrichment with few peaks in the Barnett intervals. Also notice the peaks in EF U, V and Zn in some of the Barnett samples. In Figure 3.10, the parameter %Si-excess is plotted against EF_{Mo/Al} to show Mo enrichment in the Barnett Formation relative to normal gray shale. The figure also shows that most of the Barnett Samples have excess Si.

Figure 3.11 is a chemostratigraphic plot of %TOC, TIC, %S, DOP_T, EF_{Mo/Al}, EF_{Fe/Al} and %Si-excess. This plot is used to further divide the Lower

Barnett Formation into 3 sub lithologies (Loucks and Ruppel, 2007); the argillaceous, siliceous and ferroan dolomitic facies). Figure 3.11 demonstrates increase in $EF_{Fe/Al}$, TIC increase and decrease in DOP_T values within the ferroan dolomitic facies.

The degree of bottom- water oxygenation is determined using sample DOP_T values. According to Raisewell and Berner (1988), the value cut offs for degree of pyritization is defined as follows:

- ❖ DOP_T values < 0.42 = oxic
- ❖ DOP_T values 0.46 to 0.80 = restricted
- ❖ DOP_T values > 0.55 = inhospitable, anoxic to euxinic.

The average DOP_T value for the Barnett Formation is approximately 0.7.

Enrichment factor (EF) is defined by Wedepohl (1971, 1991) as any deviation from chemical composition of average shale. $EF > 1$ means that the element is enriched relative to average shale while $EF < 1$ means that the element is depleted compared to average shale. Anoxic indicators Mo, V, U and redox sensitive element Zn is plotted against depth in Figure 3.9 and is used to show trace element enrichment of the Barnett Formation relative to average shale. Notice that the Barnett Formation is relatively enriched in Mo with few peaks in some samples; also notice the similar pattern of enrichment between V and Zn. Uranium (U) shows a zero concentration on all the Forestburg samples but few peaks on the upper and lower Barnett samples. To estimate the redox condition of

the core, sulfur(S) is plotted against total organic carbon (TOC) in figure 3.12; notice the non-positive correlation between sulfur and TOC.

3.1.3 Integrated data (Ternary Plots, organic matter composition and provenance)

The Barnett composition was compared to that of average gray shale using ternary plot of calcium oxide (CaO), alumina (Al₂O₃), and silica (SiO₂) in figure 3.14 (Wedepohl 1971, 1991). Figure 3.15 is a ternary diagram of total organic carbon (TOC), sulfur (S) and iron (Fe) used to determine the amount of Iron (Fe) held in pyrite (Dean and Arthur, 1989). Please note that all ternary plots represent the use of normalized data. The TOC elemental data in the Barnett Formation reveal significant variation ranging from 2.0 to approximately 8%.

According to Meyers, (1997) the provenance of organic matter in sediments can be identified using isotopic compositions of TOC ($\delta^{13}\text{C}$), TN($\delta^{15}\text{N}$) and Carbon/Nitrogen ratio (C/N) as shown in figure 3.16 and figure 3.17.

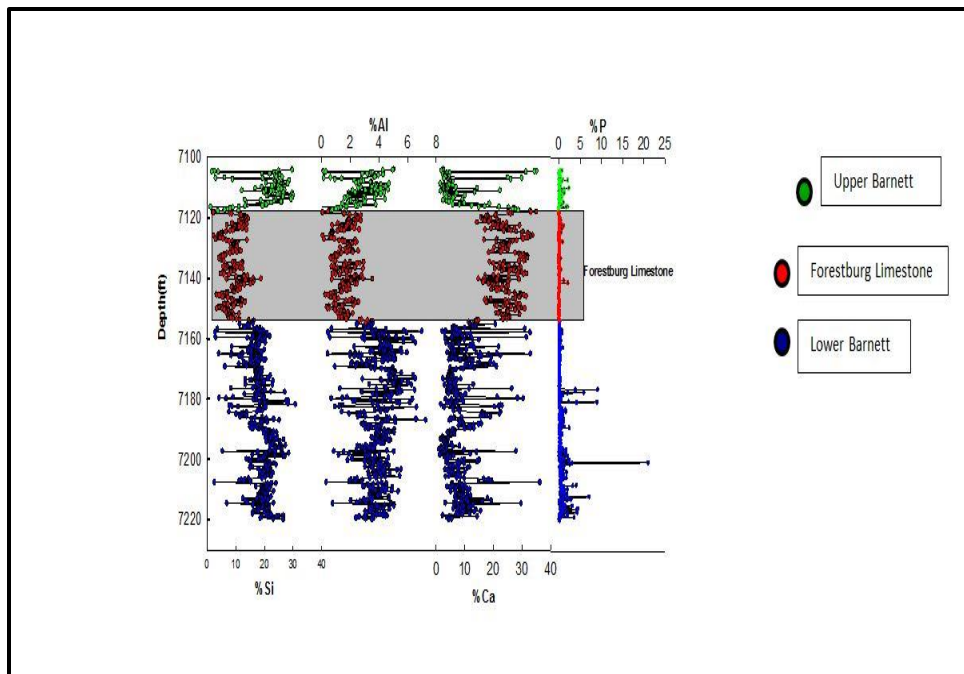


Figure 3.1 Chemostratigraphic plot of major elements (Si, Al, Ca and P), showing Forestburg interval.

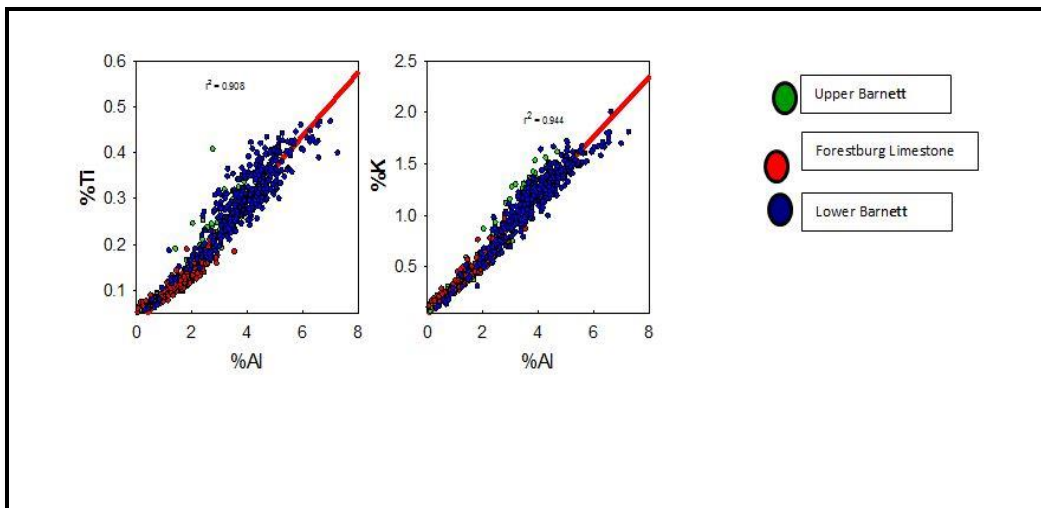


Figure 3.2 Cross-plots of Titanium (Ti) and Potassium (K) against Aluminum (Al). The red lines indicate the regression line

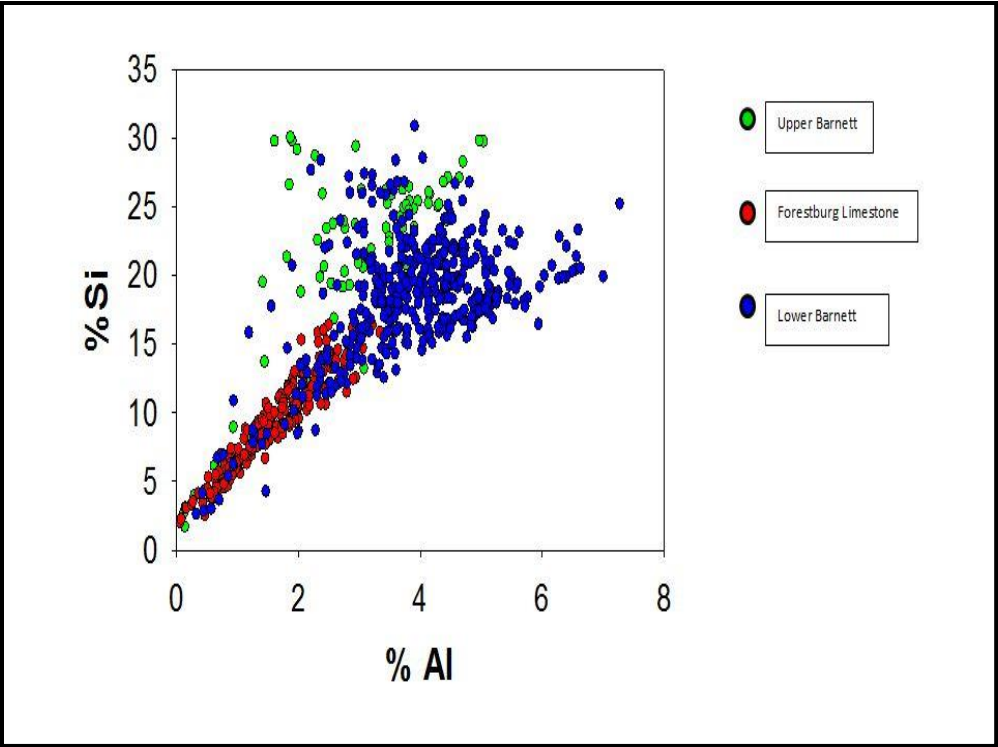


Figure 3.3 Cross-plot of Silicon (Si) against Aluminum (Al).

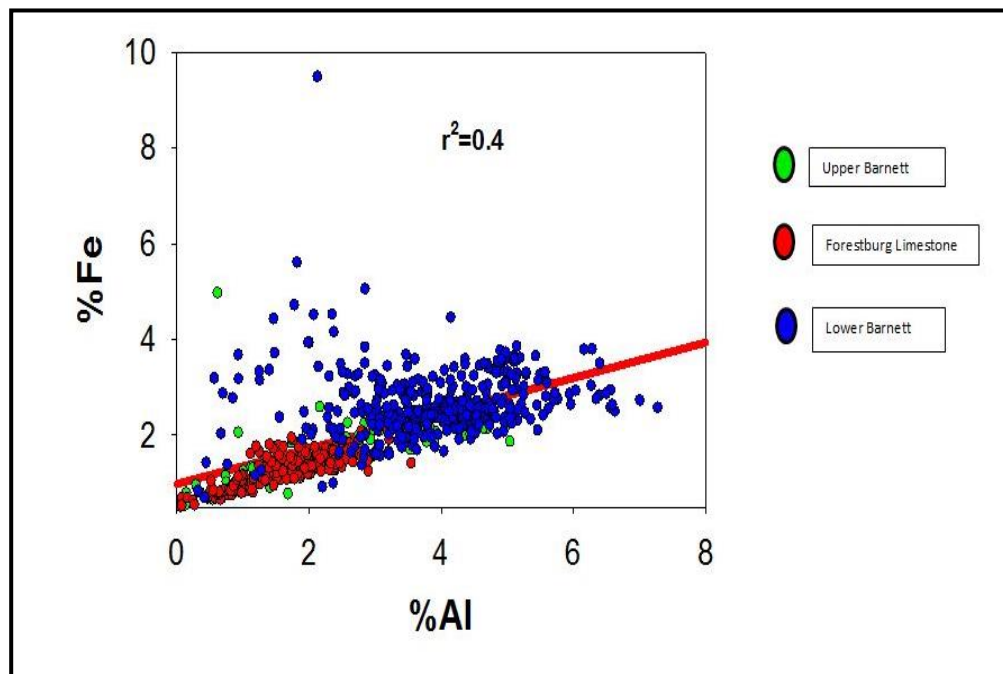


Figure 3.4 Cross-plot of Iron (Fe) versus Aluminum (Al). The red line indicates the regression line.

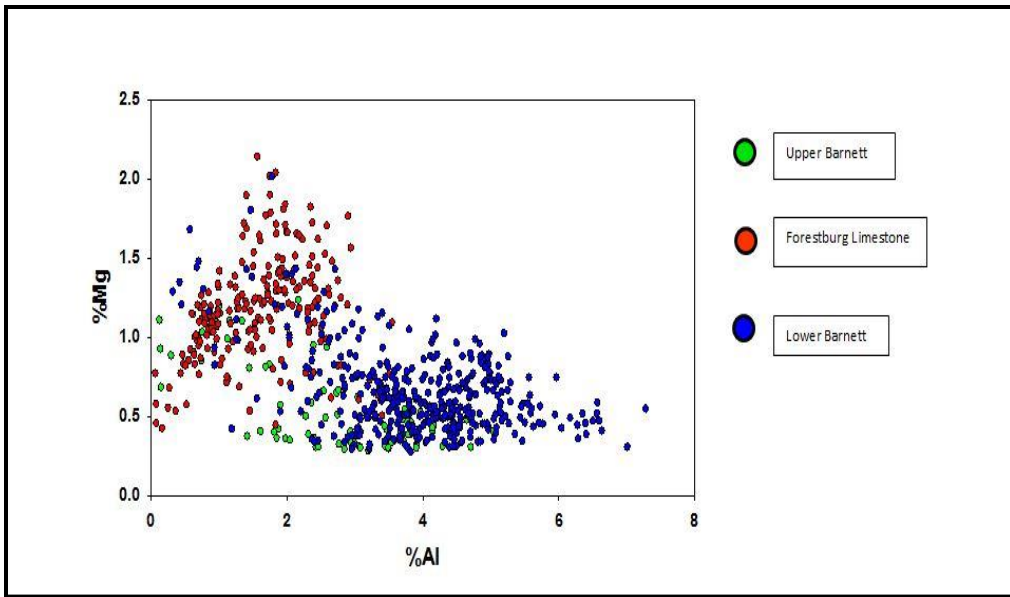


Figure 3.5 Cross-plot of Magnesium (Mg) against Aluminum (Al).

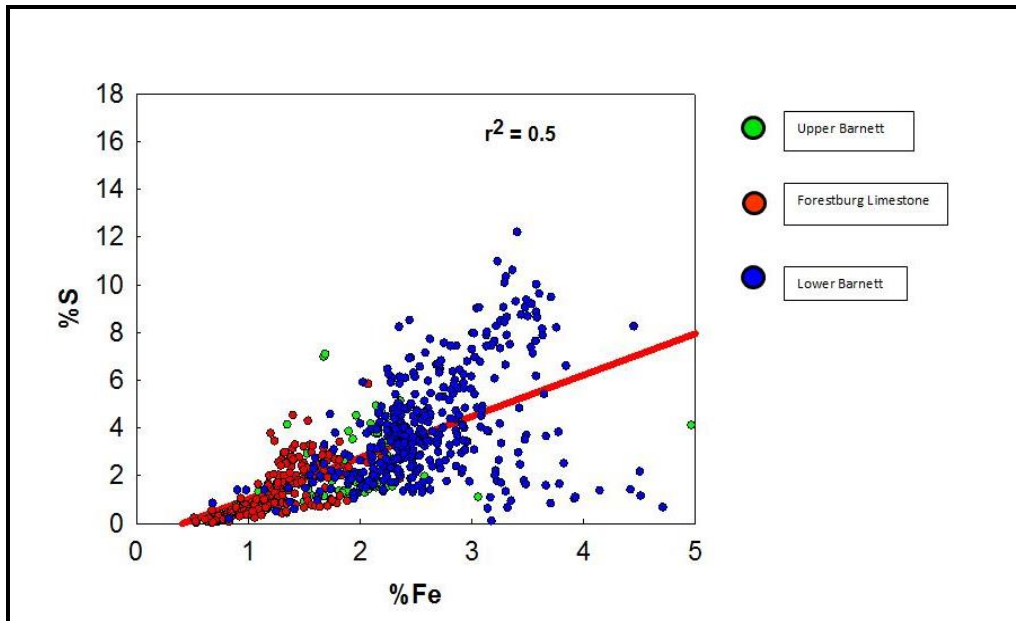


Figure 3.6 cross-plot of Sulfur (S) against Iron (Fe). The red line is the pyrite line (Fe/S ratio =1.15after Dean and Arthur, 1989)

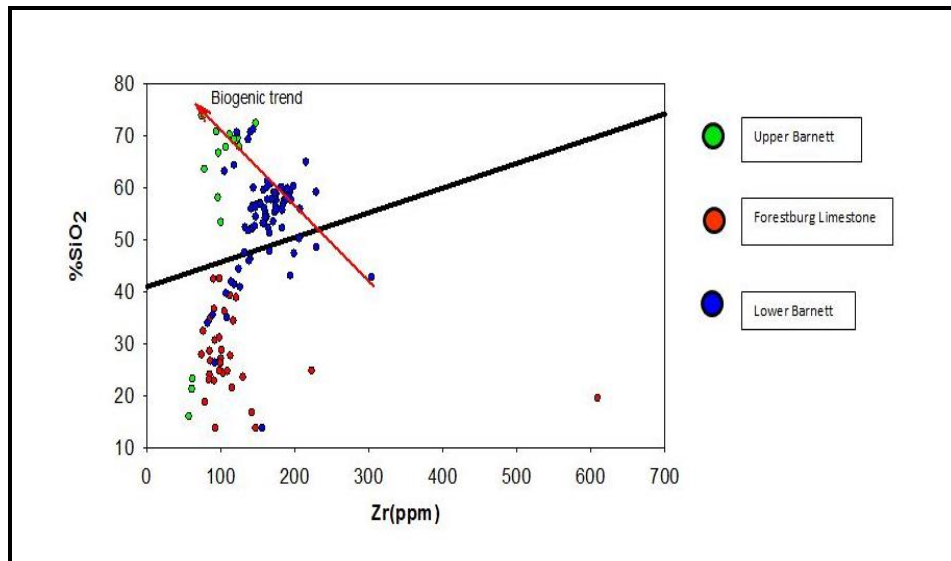


Figure 3.7 cross-plot of Silica (SiO₂) against Zircon (Zr). The red line indicates SiO₂ increase relative to Zr. The black line is the regression line.

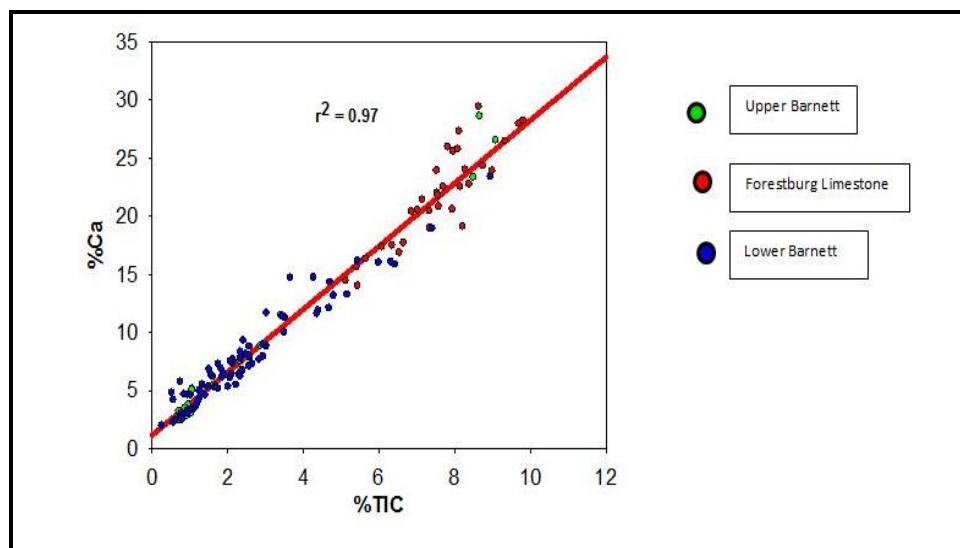


Figure 3.8 cross-plot of calcium (Ca) versus total inorganic carbon (TIC). The red line is the regression line.

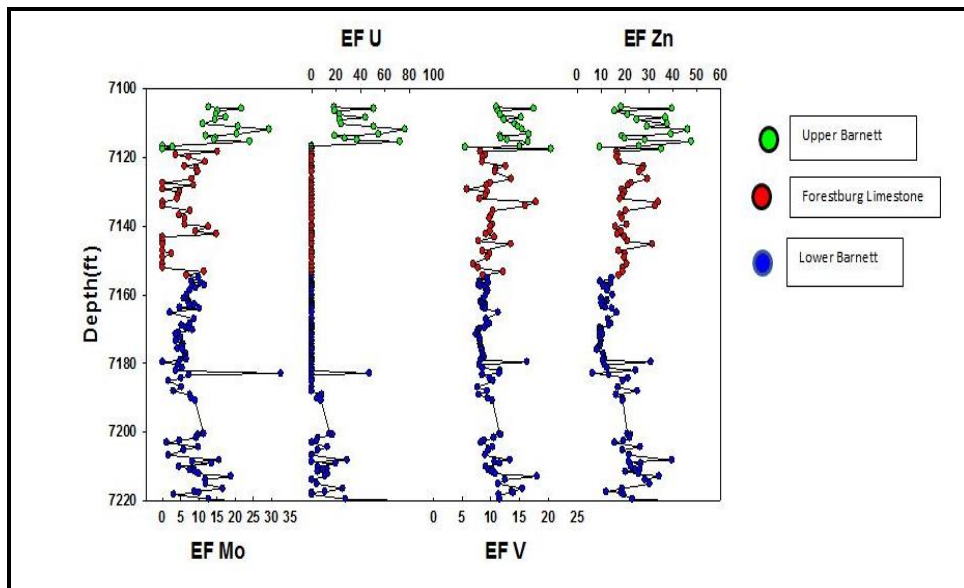


Figure 3.9 Chemostratigraphic plot of anoxic indicators; enrichment factors of molybdenum (EF Mo), uranium (EF U), vanadium (EF V) and zinc (EF Zn).

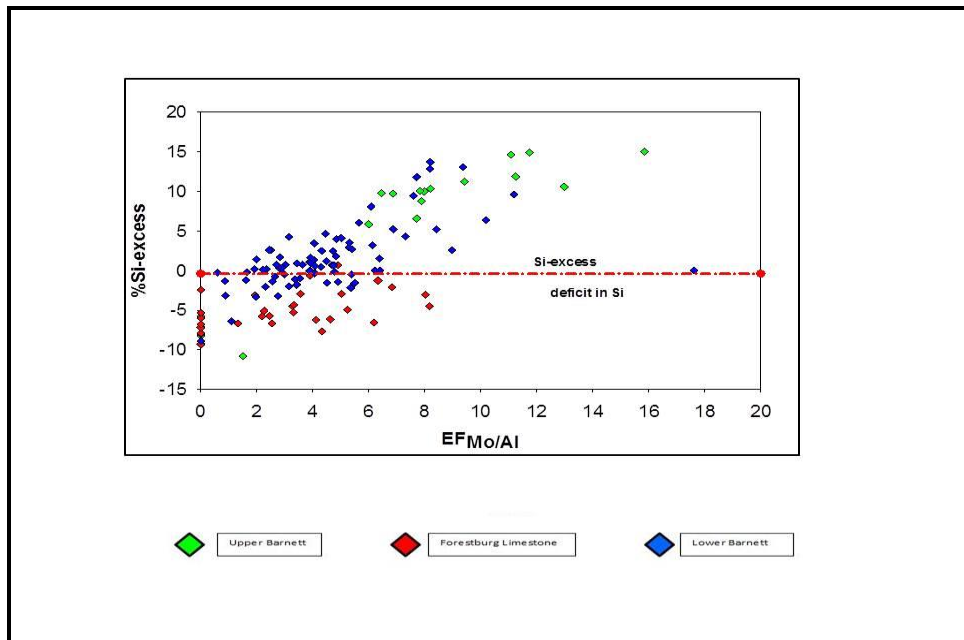


Figure 3.10 cross-plot of silicon-excess against enrichment factor molybdenum over aluminum

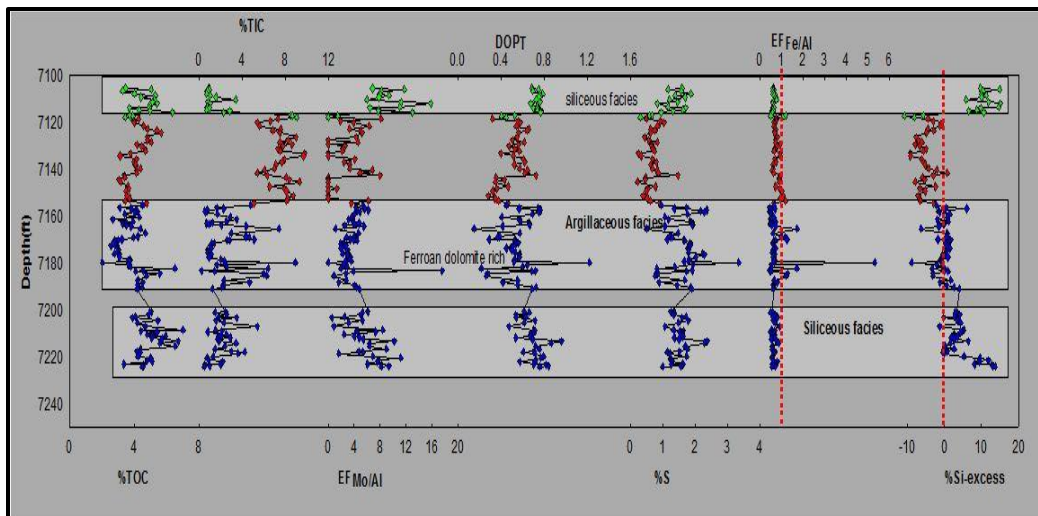


Figure 3.11 cross-plots of geochemical data with depth showing the sub-lithologies of the Barnett Formation

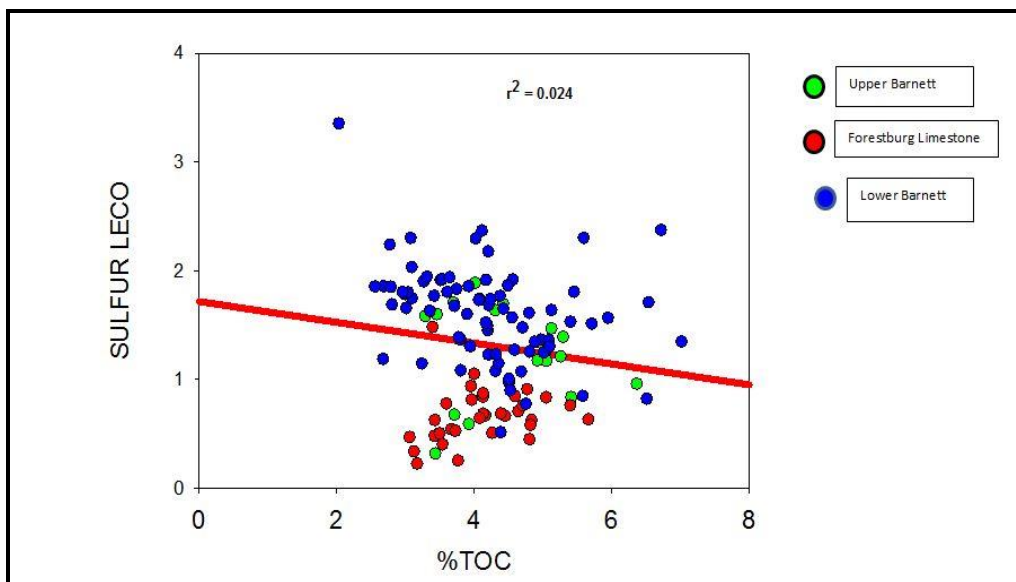


Figure 3.12 cross-plot of LECO Sulfur versus TOC. The red line represents the regression line.

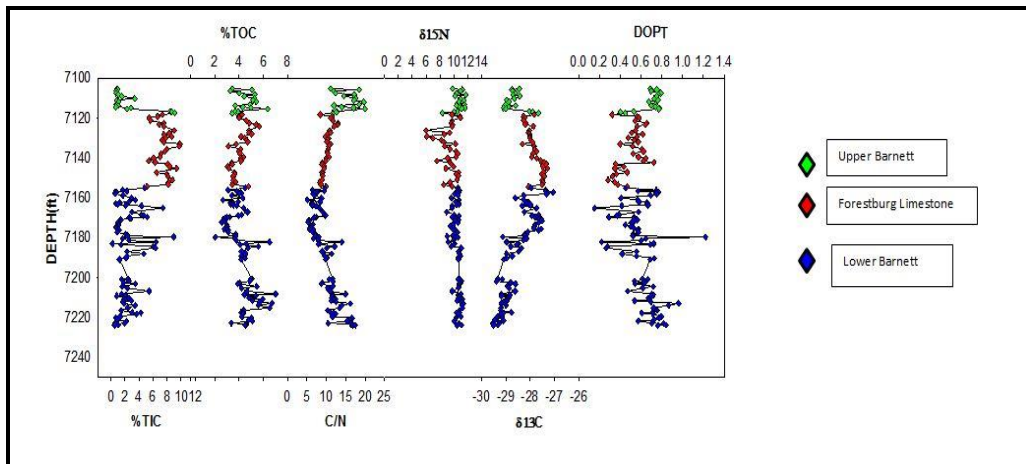


Figure 3.13 Chemostratigraphic plots of non-XRF data.

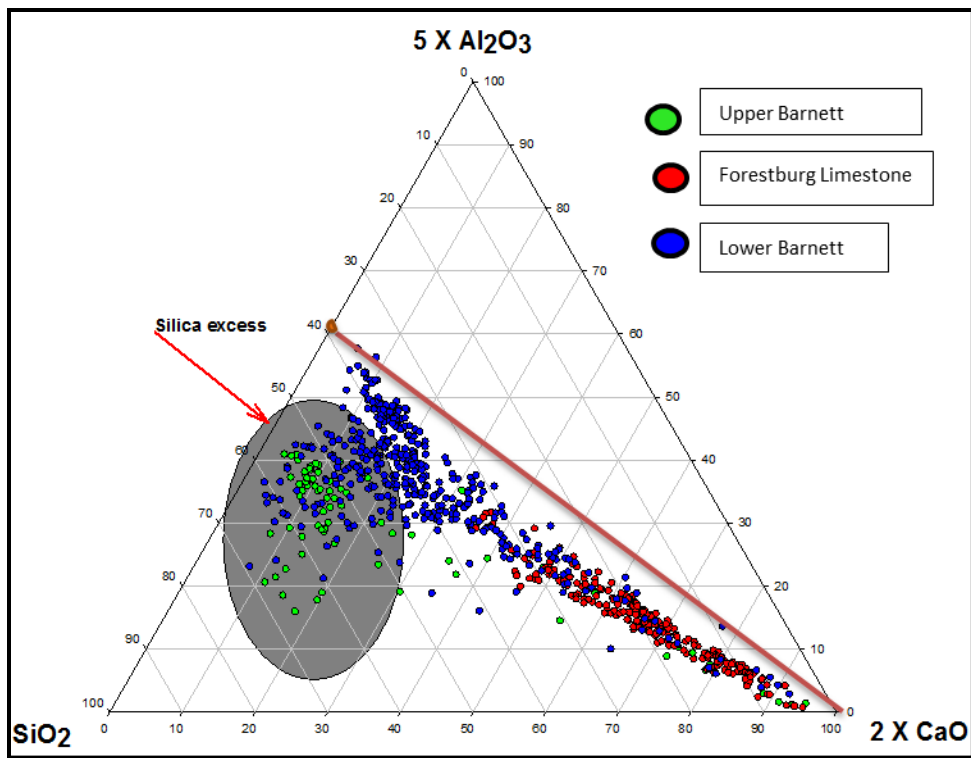


Figure 3.14 calcite-clay-quartz ternary plot for Blakely # 1. The orange line represents the calcite dilution line while the small orange circle denotes the average gray shale (Wedepohl , 1991)

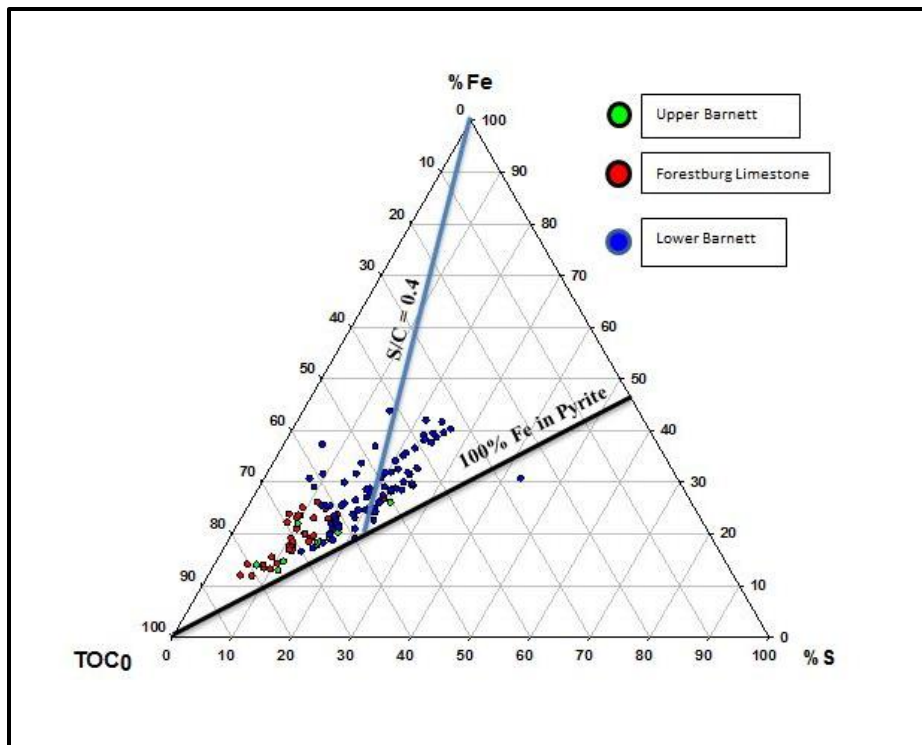


Figure 3.15 Fe-S-TOC ternary diagram of the Blakely # 1 core (after Dean and Arthur, 1989). $S/C=0.4$ represents normal marine line (NML). The black line is the pyrite line (100% Fe in pyrite)

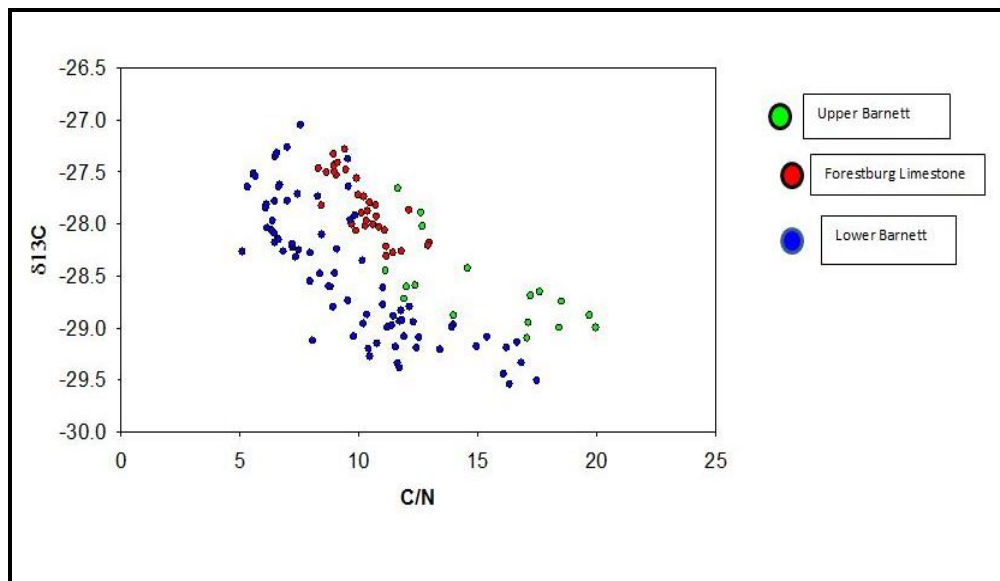


Figure 3.16 Identifier of the organic matter provenance using $\delta^{13}\text{C}$ and C/N ratio (Meyers, 1997)

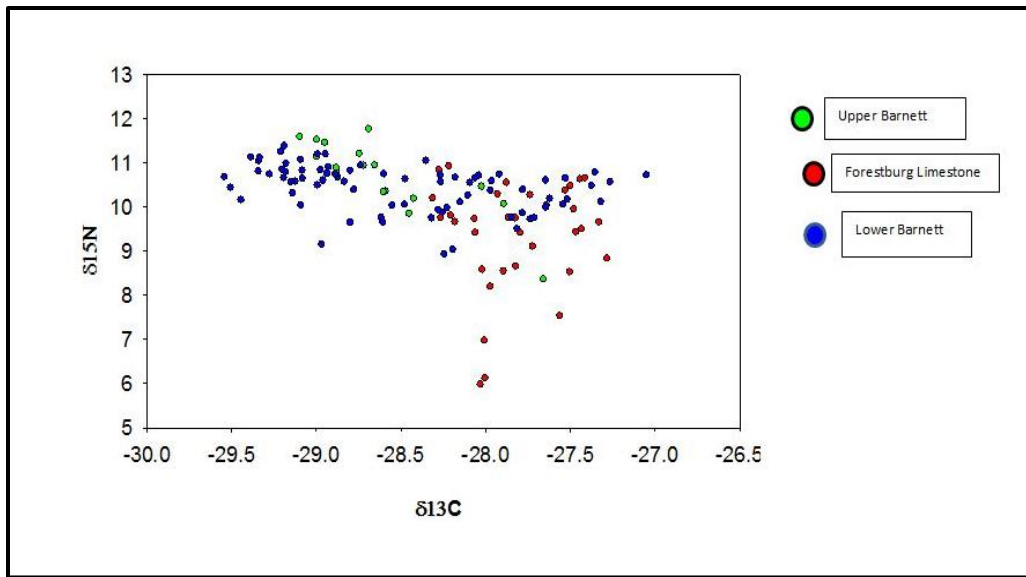


Figure 3.17 Organic matter source using $\delta^{13}\text{C}$ and $\delta^{15}\text{N}$ (Meyers, 1997).

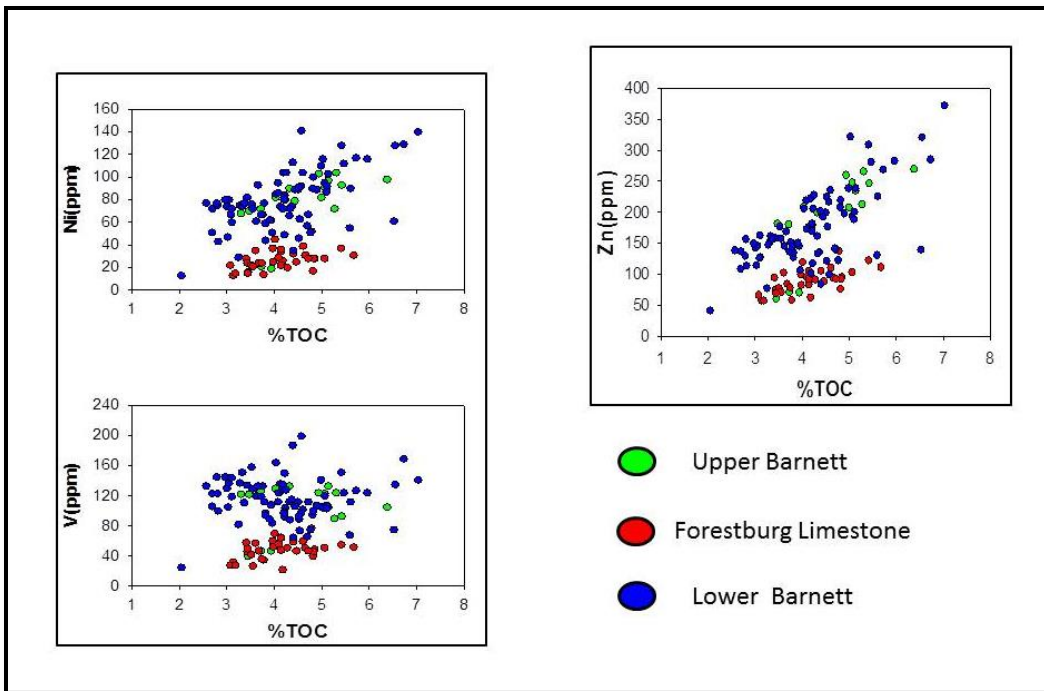


Figure 3.18 Cross-plots of trace elements versus TOC

3.1.4 Tables

Table 3.1 shows the average major elemental weight percent of the Blakely # 1 core. The cumulative average was calculated separately for each interval (the Upper Barnett, Forestburg limestone and Lower Barnett respectively). The average values for the Forestburg Limestone is not included when interpreting the Barnett Formation. The interpretative average values for the Barnett Formation used is the average values for both the Upper and Lower Barnett intervals.

Table 3.1 Average major elemental values for the Blakely # 1 core.

FORMATION MEMBER	Mg (%)	Al (%)	Si (%)	P (%)	S (%)	K (%)	Ca (%)	Ti (%)	Mn (%)	Fe (%)	V (ppm)	Cr (ppm)
Upper Barnett	0.5	4.3	27.7	0.4	1.3	0.9	9.696	0.23	0.01493	1.54	101.3	174.5
Forestburg limestone	1.2	2.7	12.9	0.1	0.7	0.5	24.157	0.12	0.01493	1.145	39.7	65.4
Lower Barnett	0.7	6.4	25.1	0.6	1.6	1.15	8.97	0.29	0.01463	3.346	136.1	183.9

Table 3.2 Average trace elemental values for the Blakely # 1 core

FORMATION MEMBER	Co (ppm)	Ni (ppm)	Zn (ppm)	Th (ppm)	Rb (ppm)	U (ppm)	Sr (ppm)	Mo (ppm)
Upper Barnett	6.0	73.9	192.5	10.1	59.9	5	368.2	10.4
Forestburg Limestone	1.2	27.5	90.1	8.8	26.3	0	675.7	2.6
Lower Barnett	9.1	79.7	175.1	10.1	74.6	1.4	558.2	8.5

Table 3.3 Average values for TOC, TIC, TN and the isotopic analysis ($\delta^{15}\text{N}$ and $\delta^{13}\text{C}$)

FORMATION MEMBER	TOC	%N	C/N	$\delta^{15}\text{N}$	$\delta^{13}\text{C}$	TIC
Upper Barnett	4.52	0.27	15.199	10.7012	-28.6035	2.6629
Forestburg Limestone	4.14	0.117787	10.207	9.3391	-27.8188	7.5542
Lower Barnett	4.23	0.41987	9.388	10.4356	-28.4847	2.4372

Chapter 4

Discussion

This chapter focuses on describing the depositional environment of the Barnett Formation in the northern part of Fort Worth Basin using the inter-elemental variations of all cross-plots described in chapter 3. The results obtained in chapter 3 is used to compared the Barnett to other shale Formations to expand our knowledge on the formation of black shale. Chemostratigraphic techniques applied to the Barnett Formation will also provide a means to characterize its lithostratigraphic unit by use of changes in its whole-rock geochemistry. To serve this purpose, the use of geochemical proxies for detrital inputs (Al, Ti, Zr, etc.), Organic association (Mo, Zn, Ni, U, Cr, etc.), Carbonates (Mg, Ca, Sr) along with TIC, TOC, isotopic compositions of TOC ($\delta^{13}\text{C}$), TN($\delta^{15}\text{N}$) and Carbon/Nitrogen ratio (C/N) will be evaluated.

4.1 Major elements and Terrigenous input

To assess the detrital input, Si/Al ratio were used to represent Quartz/Clay content. Al is generally regarded as the main conservative element used as a proxy for clay minerals in hemipelagic and pelagic sediments (Potter et al, 2004). The Si/Al ratio always reflects the abundant of silt-grade quartz in sediments and also is normally a grain size indicator (Ratcliffe et al, 2012). However, since Silica can also be associated with biogenic quartz, it is not always a detrital indicator. The good correlation between Si and Al shown in figure 3.3 suggests

that silica reside in the clay fraction. However, the silica enrichment relative to aluminum (Figure 3.3) reveals concentration of silica in non-clay minerals (e.g. quartz, feldspar). Milliken et al, 2012 studied the extent to which diagenesis affected the primary depositional controls on a core within the Barnett Formation in the eastern part of Fort Worth Basin, and noted abundant sponge spicule within the Barnett Formation. The mineral Zircon represents a proxy for silt-sized terrestrial input and is associated with Zr, while SiO₂ corresponds to the amount of quartz in the shale. Although, it is difficult to quantify the amount of biogenic quartz using whole rock geochemical data (Ratcliffe et al, 2012), samples with significant biogenic silica can be identified from geochemical data using relative proportions of SiO₂ and Zr. The relative increase in SiO₂ but decrease in Zr (non-linear relationship) observed in figure 3.7 suggests that some of the excess silica (figure 3.3) is biogenic in origin derived from sponge spicules and other silicon bearing marine organisms.

Considerable increase in calcium (Ca) concentration from approximately 7115-7155 (figure 3.1) is caused by pervasive carbonate content of the Forestburg Limestone characterized by its low gamma-ray signature and high calcite concentration (Loucks and Ruppel, 2007). Calcium also displays an inverse relationship with Silica in figure 3.1.

Titanium (Ti) and Potassium (K) are often used as detrital clay indicators, Ti is often associated with heavy mineral grains and occur both in clay and in sand grains of rutile ,augite and ilmenite (Rimmer et al,2004). High Ti/Al ratio could reflect enhanced delivery of riverine detritus (Murphy et al., 2000; Meyers et al., 2001). Increased Ti concentration relative to Al could indicate relative sea level- fall and coast line progradation (Sageman et al.,2003) or even higher eolian and volcanic ash input (Bertrand et al.,1996; Sageman et al.,2003). The strong affinity between potassium and titanium with aluminum in figure 3.2 suggests that these elements reside in the clay mineral phase possibly illite (Bowker, 2002)

Iron (Fe) shows a strong relationship with Al (figure 3.4) revealing that Fe reside in the clay mineral phase. The enrichment of Fe relative to Al particularly within the Lower Barnett samples shows that Fe resides in other mineral phase (pyrite) aside from clay. Several authors have noted the presence of pyrite mostly in framboids form within the Lower Barnett shale (e.g. Loucks and Ruppel, 2007; Papazis, 2005). Figure 3.6 shows a fairly strong correlation between Fe and sulfur (S) expressing that Fe resides in iron sulfide phase (Pyrite). However, figure 3.6 also displays some data falling to the left and right of the regression line indicating the existence of both Fe and S in other mineral phases.

Calcium (Ca) along with magnesium (Mg) and strontium (Sr) always suggest the presence of carbonates (e.g. Dolomite). Mg also occurs in clay mineral and displays the argillaceous component in the clay when associated with

Fe. Figure 3.5 shows relative enrichment in Mg in some of the Lower Barnett samples indicating dolomitic input. The strong correlation between Ca and TIC in figure 3.8 is a good geochemical proxy for carbonates suggesting that majority of the Ca is bound in the carbonate mineral phase. However, little variation in TIC concentration (figure 3.13) indicates the incorporation of other elemental constituents within the Forestburg Limestone.

The ternary plot (figure 3.14) reflects changes in clay-quartz, and calcium carbonate fractions of the Blakely # 1 core. It is used to determine the composition of the Barnett Formation relative to average marine shale (Wedepohl, 1991). All of the samples plot below the calcium dilution line (the orange line) indicating varying amount of dilution by carbonates and silica mineral phases.

4.2 Trace element and non-XRF data (TOC, TIC etc.)

Elemental concentrations of redox-sensitive trace elements such as molybdenum (Mo), vanadium (V), chromium (Cr), uranium (U) and Nickel (Ni) has been used by various researchers (Dean et al., 1997; Rimmer et al., 2004; Rowe et al., 2008, etc.) as a proxy for depositional redox conditions. These trace elements tend to be more soluble in reducing conditions and exhibit considerable enrichment in laminated organic rich facies especially those deposited under euxinic/anoxic conditions (Algeo and Maynard, 2003). Trace elements such as

Zinc (Zn), Nickel and Vanadium are micronutrients and are often connected to preserved organic matter.

Tourtelot (1979) used three models to describe the range of depositional environment in which organic rich shale may accumulate and placed great emphasis on the chemical characteristics of the environment such as the distribution of oxygen and hydrogen sulfide in the sediments and water column and also on the role of the amount of organic material in relation to oxygen supply.

Vanadium (V), zinc (Zn) and nickel (Ni) when plotted against total organic carbon (TOC) in figure 3.18 display considerable increase in concentration with TOC increase especially within the Upper and Lower Barnett samples indicating their association with preserved organic matter. These elements are typically associated with authigenic enrichment within sediments under anoxic conditions and are important indicators of anoxia.

Trace element concentration in the form of enrichment factor (EF) is also used to evaluate the redox character of the Barnett Formation. The level of enrichment is essentially expressed by comparison against “standard marine” shale (Tribovillard et al., 2006). Once calculated, EF values of 1 indicate no enrichment of an element relative to standard marine shale (meaning that the sediment was deposited in oxic conditions); whereas values EF values greater than 1 imply the elements enrichment relative to standard marine shale. Figure 3.9

shows that within the Barnett Formation, EF in excess of 1 are seen for Mo, V and Zn. These elements also display similar pattern of enrichment with molybdenum indicating anoxic-euxinic condition during the deposition of the Barnett shale.

4.2.1 Basinal restriction

The relationship of sediment Mo/TOC to hydrographic properties of modern marine systems has been used to estimate aqueous [Mo] and deep water renewal times (Algeo et al., 2007). This ratio has been applied in paleoceanographic studies of Paleozoic and Mesozoic formations by various researchers as a proxy for the degree of watermass restriction (Loucks and Ruppel, 2007 Rowe et al., 2008; Algeo and Rowe, 2011). Algeo and Rowe, (2011) pointed that lower sediment Mo/TOC ratio implies restricted and limited deep water renewal condition. The average Mo and TOC values for the Barnett Formation is 4.24 and 7.227 respectively yielding a formation average sediment Mo/TOC value of 1.7. This value suggests a high degree of watermass restriction during the deposition of the Barnett Formation.

4.2.2 Sulfur-Iron-TOC Relationship

Accumulation of organic matter in sediments is often associated with the enrichment of sulfur and Iron due to coupling of organic matter deposition to microbial sulfate reduction and the associated formation of sedimentary sulfur compounds. Dissimilatory sulfate reduction is caused by the formation of hydrogen sulfide which may further react with reactive iron to precipitate iron

sulfides (essentially pyrite) and with organic matter to form organic sulfur compounds. In marine environment, bacterial sulfate reduction is a common feature associated with organic-rich sediments and is part of the complex redox system related to organic matter oxidation (Passier and Lange, 1998).

Berner (1994) proposed that sediments deposited under oxic marine conditions yielded C_{org}/S ratio of 2.5 (normal marine line = NML) while lower C_{org}/S ratios are characteristic of euxinic environment or diagenetic pyrite formation. The average calculated values for sulfur (S) and organic carbon (C_{org}) in Barnett samples analyzed are 3.043565 and 4.375 respectively, yielding an average formation C_{org}/S ratio of 1.4 indicating euxinic environments.

The non-positive correlation and the positive intercept between sulfur and TOC in figure 3.12 also indicate that the Barnett Formation was accumulated under anoxic or euxinic condition (based on Berner and Raiswell, 1983). Recognition of iron-carbon-sulfur limitation on pyrite formation is possible by the ternary plot (figure 3.15) after Dean and Arthur (1989). Data concentration along a line of constant S/Fe ratio (pyrite line) indicate Fe limitation on pyrite formation. The constant $Fe/S = 1.15$ (stoichiometric pyrite after Dean and Arthur, 1989) when all iron is reactive. The regression line through the data point of constant S/Fe ratio shifts towards the Fe corner when only a portion of the total iron is reactive. The average S/Fe ratio for the lower Barnett Formation is approximately 0.68 indicating that at least 60% of the total iron is held in pyrite

form. Concentration of data along the normal marine line ($S/C = 0.4$) in figure 3.15 would indicate carbon limitation (adopted by Berner, 1982). Samples with only pyritic sulfur cannot have S/Fe ratio below 1.15 (Dean and Arthur, 1989). Thus, the average S/Fe ratio (0.68) of the Lower Barnett samples is an indication of additional form of sulfur (e.g. organic sulfur).

4.2.3 Degree of Pyritization (DOP)

The degree of pyritization as previously stated in chapter 3 is the ratio of pyritic iron to the total iron (Raiswell and Berner, 1988). It is often used as a proxy for paleoenvironmental and redox state of bottom waters and can also be used to demonstrate iron or sulfur limitation in pyrite formation (Dean and Arthur, 1989). Framboidal pyrite is formed at the oxic-anoxic transition by replacement of more sulfide rich phases in euxinic bottom waters (Wilkin et al., 1996). During early diagenesis, the majority of pyrite precipitates as spherical framboids formed by aggregation of submicron sized individual particles, or as single or clustered euhedral crystals (Wilkin et al., 1996). Wilkin and others have used the size and texture of pyrite to differentiate syngenetic and diagenetic pyrite and thereby account for bottom water oxygen conditions (Wilkin et al., 1996; Wignall and Newton, 1998).

Based on a comprehensive analysis of ancient shale formations proposed by Raiswell et al. (1988), sample DOP_T values between 0.46 and 0.75 indicate restricted condition while sample DOP_T values greater than 0.55 suggest

inhospitable euxinic environment. The calculated average DOP_T value for the Upper and Lower Barnett samples is approximately 0.7. Figures 3.11 and 3.13 also display that majority of the Barnett samples plot in the restricted/inhospitable field (indicating the absence of oxygen and potential presence of hydrogen sulfide).

4.2.4 Organic matter composition and provenance

The organic aspect of the Barnett Formation in the northern end of Fort Worth basin will be examined in this section using total organic carbon (TOC), stable isotopes of organic carbon and carbon nitrogen ratio. The Barnett in the northern part of Fort Worth Basin is relatively rich in organic carbon with TOC values ranging from 2.0 to approximately 8.0 with formation average TOC value of 4.4.

The accumulation and preservation of significant amount of organic matter in sediments requires specific conditions in the sedimentary environments. The role of the amount of organic material in relation to oxygen supply cannot be over-emphasized when describing the conditions in which organic rich shale accumulate in sedimentary basins. Thus, the restricted circulation model proposed by Tourtelot,(1979) presents a classic view of the accumulation of organic material in ancient rocks. This model explains that the oxygen content of the water column is not renewed by circulation so that organic rich sediments can accumulate even if the organic productivity is relatively small (Tourtelot, 1979).

Marine environment with high bio-productivity in the surface waters and oxygen deficiency in bottom waters favors elevated organic carbon content in sediments.

The oxygen depletion may have been caused by large oxygen demand of the decomposing organic material itself. This depletion in oxygen may lead to anaerobic decomposition of the organic matter and hydrogen sulfide formation mainly because of the little circulation in the water mass to supply oxygen at a rate fast enough to equal oxygen demand of the organic materials, so both the sedimentary environment and the sediments are anoxic (Tourtelot, 1979). Excess in silica composition particularly within the Upper interval of the Barnett Formation (figure 3.10) is also a proxy for high organic productivity within the Barnett Formation. Milliken et al., 2012 noted the abundance of organic materials (e.g. sponge spicules, radiolarian fragments) and its replacement by authigenic minerals particularly quartz, ferroan dolomite and pyrite within the Barnett Formation.

In this context, the organic richness of the Barnett samples is likely because of high primary productivity with intense preservation of organic matter associated with low oxygen levels in the bottom waters. The presence of biogenic silica (Milliken et al., 2012) within the Barnett Formation might also be related to the diagenetic transformation of smectite to illite producing authigenic quartz.

Organic matter province of the Barnett Formation was also examined using organic carbon isotopes ($\delta^{13}\text{C}$) and C/N ratios developed by

Meyers, (1997) who proposed that variations in proportions of marine versus terrigenous organic matter sources can alter the carbon isotopes of bulk organic matter and that organic matter origin can be determined using C/N ratios. C/N ratios < 10 indicate an origin of organic matter from marine algae whereas terrigenous organic matter yields C/N ratios >20 (Meyers, 1997). Organic matter produced by land plants has an average $\delta^{13}\text{C}$ value of approximately -27‰ whereas marine organic matter has an average $\delta^{13}\text{C}$ between -20‰ to -22‰ (Meyers, 1997).

The $\delta^{13}\text{C}$ for the Upper Barnett interval has an average value of -27.8‰ whereas the Lower Barnett interval has an average of -28.5‰ making a formation average of approximately -28‰ . These values range from -27‰ to approximately -30‰ .

The average C/N ratio for the Upper and Lower Barnett interval is 8.4 and 7 respectively, making a formation average ratio approximately 9. The C/N ratio for both the Upper and Lower Barnett interval range from 5 to 20 indicating that the organic matter is more marine in origin than terrestrial. The lack of terrestrial organic matter input could result from the geographic isolation of Fort Worth basin during the Barnett deposition (Algeo and Rowe, 2012). Previous study of the organic geochemistry of the Barnett Formation also indicates a marine origin for the present organic carbon (Bruner and Smosna, 2011).

The $\delta^{13}\text{C}$ analysis yielded high negative values than would expect for marine origin. Diagenesis and environmental parameters have been noted to alter

the carbon isotopic signatures of systems heavily dominated by marine productivity, leading to $\delta^{13}\text{C}$ enrichment or depletion in the residual organic matter (Rau et al., 1989; Macko and Engel, 1993). Bacterial methanogenesis (the formation of methane by microbes) has also been documented as a possible cause of $\delta^{13}\text{C}$ enrichment in marine sediments (Whiticar, 1999). The $\delta^{13}\text{C}$ enrichment could possibly be explained by the strong diagenetic overprint within the Barnett Formation (Milliken et al., 2012).

Chapter 5

Conclusions

The integration of geochemical proxies has provided insight into the depositional history of the Barnett Formation during the mid-late Mississippian time. Elemental concentrations and ratios were also useful in defining stratigraphic shifts in mineralogy, paleo-redox condition and sedimentation in the Fort Worth Basin during the deposition of Barnett Formation in Wise County Texas. Stable isotopes of carbon and carbon nitrogen ratio provided clue into the provenance of organic matter that accumulated within the Barnett Formation.

Chemostratigraphic/elemental analysis of the Blakely #1 core of the Barnett Formation demonstrated :

- ❖ The Barnett Formation is composed primarily of siliceous and calcareous mudstone with significant amount of pyrite and phosphate mineral phases
- ❖ Some of the excess-silica present in the Barnett Formation is biogenic in origin, based upon relative proportions of SiO₂ and Zr.
- ❖ A high degree of water mass restriction in the Fort Worth basin during the deposition of Barnett Formation (based upon Mo/TOC relationship).
- ❖ The Barnett Formation is rich in organic matter with a formation average TOC value of 4.4. The organic matter provenance was

determined to be primarily of marine origin based on the C/N ratio, degree of hydrographic restriction and previous organic geochemistry research done by other geoscientists.

- ❖ The redox conditions were mostly anoxic-euxinic during the Barnett Formation deposition based upon high TOC, presence of pyrite, trace element enrichment and degree-of-pyritization (DOP) values modeled.

References

- Algeo, T.J., and Maynard, J.B., 2003. Trace-element behavior and redox facies in core shales of Upper Pennsylvanian Kansas-type cyclothems. *Chemical Geology*. 206: p.289-318.
- Algeo, T.J., Lyons, T.W., Blakey, R.C., Over, D.J., 2007. Hydrographic conditions of the Devonian-Carboniferous Seaway inferred from sedimentary Mo-TOC relationships. *Paleogeography, Paleoclimatology, Paleoecology* 256; p.204-230.
- Algeo, T.J. and Rowe, H.D., 2011. Paleooceanographic, applications of trace-metal concentration data. *Chemical Geology* article, vol.324-325.p.6-18.
- Alplin, A.C., Fleet, A.J., and Macquaker, J.H., 1999. Muds and Mudstones: physical and fluid flow properties. Geological Society London, special publications, vol.158. P.1-8.
- Andrew, A.S., Whitford, D.J., Hamilton, P.J., 1996. Application of chemostratigraphy to petroleum exploration and field appraisal: An example from the Surat Basin, Society of Petroleum Engineers, Document ID 37008-MS, SPE Asia Pacific Oil and Gas Conference, 28-31 October 1996, Adelaide, Australia, 978-1-55563-419-3.
- Berner, R.A., 1982. Burial of organic carbon and pyrite sulfur in the modern ocean: its geochemical and environmental significance, *American Journal of Science* 282, p.451-473.
- Berner, R.A. and Raiswell, R., 1983. Burial of organic carbon and pyrite sulfur in sediments over Phanerozoic time: a new theory, *Geochimica et Cosmochimica Acta* Vol. 47, p.855-862.
- Berner, R.A. and Raiswell, R., (1984): C/S method for distinguishing freshwater from marine Sedimentary rocks. *Geology*, 12, p.365-368.
- Berner, R.A., 1994. Geocarb II: A revised model of the atmospheric CO₂ over Phanerozoic time. *American Journal of Science* :294.p.56-91.

Bertrand, P., Shimmield, G., Martinez, P., Grousset, F., Jorissen, F., Paterne, M., Pujol, C., Bouloubassi, I., Buat Menard, P., Peypouquet, J.P., Beaufort, L., Sicre, M.A., Lallier-Verges, E., Foster, J.M., Ternois, Y., 1996. The glacial ocean productivity hypothesis: the Importance of regional temporal and spatial studies. *Marine. Geology*:130, p.1 –9.

Bowker, K. A., 2002, Recent developments of the Barnett Shale play, Fort Worth Basin, in B. E. Law and M. Wilson, eds., *Innovative Gas Exploration Concepts Symposium: Rocky Mountain Association of Geologists and Petroleum Technology Transfer Council*, October, Denver, Colorado, p.16.

Blakey, R., 2005. Paleogeography and geologic evolution of North America; images that track the ancient landscapes of North America. online : <http://jan.ucc.nau.edu/~rcb7/nam.html> (accessed Nov. 2012).

Brunner, K., and Smosna, R., 2011, *A Comparative Study of the Mississippian Barnett Shale, Fort Worth Basin, and Devonian Marcellus Shale, Appalachian Basin* : US department of Energy 2011 .

Curtis, J.B., 2002. Fractured shale-gas systems. *AAPG Bulletin*. November, 2002, V.86.no.11.p.1921-1938.

Crusius, J., Calvert, S., Pedersen, T., Sage, D., 1996. Rhenium and molybdenum enrichments in sediments as indicators of oxic, suboxic and sulfidic conditions of deposition. *Earth and Planetary Science Letters*. 145: p.65–78.

Dean, W.E. and Arthur, M.A. 1989. Iron–sulfur–carbon relationships in organic-carbon-rich sequences I: Cretaceous western interior seaway. *American Journal of Science*. 289: p.708–743.

Dean, W. .E., Gardner, J.V., Piper, D.Z., 1997. Inorganic geochemical indicators of glacial-interglacial changes in productivity and anoxia on the California continental margin. *Geochim. Cosmochim. Acta* 61; 4507-4518.
Demaison, G.J. and Moore, G.T. 1980. Anoxic environments and oil source bed genesis. *American Association of Petroleum Geologists Bulletin*. 64: p.1179–1209.

Didyk, B.M., Simoneit, B.R.T., Brassell, S.C., Eglinton, G., 1978. Organic geochemical indicators of palaeoenvironmental conditions of sedimentation. *Nature*, 272: 216-222.
Diessel, C.F.K., (1992): *Coal bearing depositional systems*. Springer, Berlin, p.721

Flawn, P.T, Goldstein A, King, P.B, and Weaver, C.E., 1961.the Ouachita system: Texas University, Bureau of Economic Geology .Publ.6120, p.401.

Flippin, J. W., 1982.The stratigraphy, structure, and economic aspects of the Paleozoic strata in Erath County, north central Texas, in C. A. Martin, ed., Petroleum geology of the Fort Worth Basin and Bend arch area: Dallas Geological Society, p. 129–155.

Grayson, R. C. Jr., G. K. Merrill, M. J. Pranter, and L. L. Lambert, 1991.Carboniferous geology and tectonic history of the southern Fort Worth (foreland) Basin and Concho platform, Texas: Dallas Geological Society, Dallas, Texas, Field Trip No. 13, p.67 .

Hayden, J., and Pussel, D., 2005. The Barnett shale, visitors guide to the hottest gas play in the USA: Pickering Energy Partners Inc.

Heckel,P.H.,1977.Origin of phosphatic black shale facies in Pennsylvanian cyclothems of mid-continent North America AAPG Bulletin, July 1977, v. 61, p. 1045-1068

Heckel, P.H., 1991. Thin widespread Pennsylvanian black shales of Midcontinent North America: A record of cyclic succession of widespread pycnoclines in fluctuating Epeiric Sea: *Geological Society, London, Special Publications*, 1991, no.58 p.259-273.

Henry, J. D., 1982, Stratigraphy of the Barnett Shale (Mississippian) and associated reefs in the northern Fort Worth Basin; in C. A. Martin, ed., Petroleum geology of the Fort Worth Basin and Bend arch area: Dallas Geological Society, p. 157– 178.

Hodgden , J., and Martin, C.A., 1974, Fort Worth basin very busy again: the oil and gas jour.,Nov.2,p.244-251.

Ingersoll, **R.V.**, Dickinson, G., Himalayan-Bengal Model for Flysch Dispersal in Appalachian-Ouachita system: Geological Society of America Bulletin, vol. 86, p. 273-286

Jarvie, D.M., Hill, R.J., Ruble, T.E., and Pollastro, R.M.2006, 2007. Unconventional shale-gas systems: The Mississippian Barnett Shale of north-

central Texas as one model for thermogenic shale-gas assessment. AAPG Bulletin. vol. 91, no. 4. p. 475–499.

Jurdy, D.M., Stefanick, M., Scotese, C.R., 1995. Paleozoic plate dynamics. Journal of Geophysical Research. 100(B9), 17:965–975.

Kane, J., 2006 . Petrophysical characterization of Barnett shale. Bureau of Economic Geology, PBGSP annual meeting, 2006.

Kerans, C., 1988. Karst-controlled reservoir heterogeneity; Ellenburger Group Carbonates West Texas: AAPG Bulletin, v. 7.

Kier, R.S., McBride E.F., 1979, the Mississippian and Pennsylvanian system in United States : USGS. paper 1110-S.

Kier, R. S. 1988. Paleozoic strata of the Llano region, Central Texas: Geological Society of America Centennial Field Guide – South – Central Section, v. 6, p. 351-360.

Loucks, R.C., Ruppel, S.C., 2006, 2007. Mississippian Barnett shale : lithofacies and depositional setting of a deep-water shale-gas succession in Fort Worth basin , Texas: AAPG Bulletin, v.91, no.4, p.579-601.

Loucks, R.G., Reed, R.M., Ruppel, S.C., Jarvie, D.M., 2009. Morphology, genesis and distribution of nanometer-scale pores in siliceous mudstones of Mississippian –Barnett shale. Journal of sedimentary research. 79, p.848-861.

Macko, S.A., Engel, M.H., 1993. Organic geochemistry: principles and applications. New York, London: plenum press. p.699-738.

Mapel, W. J., R. B. Johnson, G. O. Bachman, and K. L. Varnes, 1979. Southern midcontinent and southern Rocky Mountains region, in L. C. Craig and C. W. Connor, coordinators, Paleotectonic investigations of the Mississippian system in the United States: U. S. Geological Survey Professional Paper, v. P 1010, p. 161–187.

McBee, W. Jr., 1999. Regional paleo-geography and geology of the southern midcontinent, in D. T. Grace and G. D. Hinderlong, eds., The Permian Basin: Providing energy for the future: West Texas Geological Society Publication 99-106, p. 139–158.

- Meyers, P.A., 1997. Organic geochemical proxies of paleoceanographic, paleolimnologic, and paleoclimatic processes, *Permagon, Org. Geochem.* Vol.276, No. 5/6; p.213-250.
- Milliken, K.L., Esch, W.L., Reed, M.R and Zhang, T. , 2012 .Grain assemblages and strong diagenetic overprinting in siliceous mudrocks, Barnett shale Fort Worth Basin : AAPG bul.2012.
- Montgomery, S. L., D. M. Jarvie, K. A. Bowker, and R. M. Pollastro, 2004, 2005. Mississippian Barnett Shale, Fort Worth Basin: Northcentral Texas: Gas-shale play with multi-tcf potential: AAPG Bulletin, v. 89, p. 155–175.
- Murphy, A.E., Sageman, B.B., Hollander, D.J., Lyons, T.L., Brett, C.E., 2000. Black shale deposition and faunal overturn in the Devonian Appalachian Basin: clastic starvation, seasonal water column mixing, and efficient biolimiting nutrient recycling *Paleoceanography* 15; p.280-291.
- Oschmann, W., 1991, 1988. Kimmeridge Clay sedimentation – a new cyclic model. *Palaeogeography, Palaeoclimatology, Palaeoecology* 65; p. 217-251
- Papazis, P.K. 2005. Petrographic characterization of the Barnett Shale, Fort Worth Basin, Texas. Master's thesis: University of Texas at Austin. p. 142.
- Passier, L., and Lange, G.J., 1998. Sedimentary sulfur and iron chemistry in relation to the formation eastern Mediterranean sapropels. *proc. ODP, sci. results.* vol.160
- PI Dwight CD., 2012. Texas and Oklahoma well data vol.22.issue 10
- Plummer, F.B. and Moore, R.C., 1921. Stratigraphy of the Pennsylvanian formations of north-central Texas. *University of Texas bull.* 2132.p 237
- Pollastro, R. M., 2003, Geologic and production characteristics utilized in assessing the Barnett Shale continuous (unconventional) gas accumulation, Barnett-Paleozoic total petroleum system, Fort Worth Basin, Texas: Barnett Shale Symposium, Ellison Miles Geotechnology Institute at Brookhaven College, Dallas, Texas, November 12–13, 2003, p.6.
- Pollastro, R.M., Hill, R.J., Jarvie, D.M., Henry, M.E., 2003 . Assessing Undiscovered Resources of the Barnett-Paleozoic Total Petroleum System, Bend

- Arch–Fort Worth Basin Province, Texas. Search and Discovery Article #10034 (2003).
- Pollastro, R. M., 2007, Total petroleum system assessment of undiscovered resources in the giant Barnett Shale continuous (unconventional) accumulation, FortWorth Basin,Texas: AAPG Bulletin, v. 91, p. 551–578.
- Potter,P.E., Maynard,J.B .,Depetris,P.J.,2004.Mud and Mudstones : introduction and overview. ISBN 3-540-22157-3
- Raiswell, R. and Berner, R.A. 1986,1988. Pyrite and organic matter in Phanerozoic normal marine shales. *Geochimica et Cosmochimica Acta*. 50: 1967–1976.
- Raiswell, R., Buckley, F., Berner, R.A., and Anderson, T.F. 1988. Degree of pyritization of iron as a paleoenvironmental indicator of bottom-wateroxygenation. *Journal of Sedimentary Petrology*. 58: p.812–819
- Rankin, D.W., 1976, Appalachian salient and recesses: late Precambrian continental breakup and the opening of the lapetus ocean: *Jour .Geoph. Res* v.81, p.5605-5619.
- Rimmer, S.M., 2004. Geochemical paleoredox indicators in Devonian-Mississippian black shales, Central Appalachian Basin (USA). *Chemical Geology*, 206; p.373-391.
- Rimmer, S.M., Thompson, J.A., Goodnight, S.A., Robl,T.L, 2004. Multiple controls on the preservation of organic matter in Devonian-Mississippian marine black shales: geochemical and petrographic evidence. Elsevier Publication, *Paleogeography, Paleoclimatology, Paleoecology* 215;p. 125-154.
- Ratcliffe, K. and Wright, K., 2012. Unconventional methods for unconventional plays : using elemental data to understand shale resource plays. Part 1 and 2.Pessa news resources.
- Rau, G.H.,Takahashi, T.,Des Marais, J.,1989. Latitudinal variations in plankton $\delta^{13}\text{C}$: implications for CO_2 and productivity in the past oceans.*Nature*,341,p.516-518
- Ross, C. A. and Ross, J.R.P. 1987. Late Paleozoic sea levels and depositional sequences, in C. A. Ross and D. Haman, eds., *Timing and deposition of eustatic*

sequences: Constraints on seismic stratigraphy: Cushman Foundation for Foraminiferal Research Special Publication. 24: 137– 149.

Rousseau, R. M. 2001. Detection limit and estimate of uncertainty of analytical XRF results.

Rowe, H.D., Loucks, R.G., Ruppel, S.C., Rimmer, S.M., 2008. Mississippian Barnett Formation, Fort Worth Basin, Texas: Bulk geochemical inferences and Mo-TOC constraints on the severity of hydrographic restriction, Elsevier, *Chemical Geology* 257; p.16-25

Rowe, H.D., Hughes, N., 2010. Strategy for developing and calibrating shale and mudstone chemostratigraphies using hand-held X-ray fluorescence units. AAPG Poster presentation.

Sageman, B.B, Murphy, A.E, Werne, J.P, Ver Straeten, C.A, Hollander, D.J and Lyons, T.W., 2003. A tale of shales: the relative roles of production in the accumulation of organic-rich strata, Middle-Upper Devonian, Appalachian basin. *Chemical Geology* 195; p.229-273.

Sageman, B.B, Murphy, A.E, Werne, J.P, Ver Straeten, C.A, Hollander, D.J and Lyons, T.W. 2003. A tale of shales: the relative roles of production in the accumulation of organic-rich strata, Middle-Upper Devonian, Appalachian basin. *Chemical Geology* 195; p.229-273.

Sageman, B.B., Lyons, T.W., 2003. Geochemistry of fine-grained sediments and sedimentary rocks. In: MacKenzie, F. (Ed.), *Treatise on Geochemistry* 7. Elsevier Publishing; p. 115-158.

Thompson, D.M., 1988. Fort Worth Basin in Montgomery: AAPG bulletin vol.89 no.2 p.151-157

Thomas, J.D., 2002, integrating synsedimentary Tectonics with sequence stratigraphy to understand the development of Fort Worth basin: AAPG Search and Discovery Article #90023.p.149-157

Tribovillard, N., Algeo, T.J., Lyons, T., Riboulleau, A., 2006. Trace metals as paleoredox and paleoproductivity proxies: An update, Elsevier, *Chemical Geology* 232; 12-32.

Turner, G.L., 1957, 1958. Paleozoic stratigraphy of Fort Worth basin: Fort Worth Geol. Socie., 1957 p.57-77

Tourtelot, H.A., 1979. Black shale-its deposition and diagenesis. Clay and clay minerals. vol.27, no.5, p 313-321.

Walper, J.L and Rowlett, C.L., 1972. Plate tectonic and origin of the Caribbean sea and the Gulf of Mexico: Gulf Coast Assoc.Geol.v.22.p.105-116

Walper, J.L., 1977. Paleozoic tectonics of the southern margin of North America: Gulf Coast Assoc. Geol. v.27. p230-241

Walper, J. L., 1982, Plate tectonic evolution of the Fort Worth Basin, in C. A. Martin, ed., Petroleum geology of the Fort Worth Basin and Bend arch area: Dallas Geological Society, p. 237–251.

Wedepohl, K.H., 1971, 1991. Environmental influences on the chemical composition of shales and clays. In: Ahrens, L.H., Press, F., Runcorn, S.K., Urey, H.C. (Eds.), Physics and Chemistry of the Earth vol. 8, Pergamon, Oxford (1971), p. 305–333.

Whiticar, M.J. 1999. Carbon and hydrogen isotope systematics of bacterial formation and oxidation of methane. Chemical Geology. 161: p.291-314.

Wilkin, R.T., Barnes, H.L., and Brantley, S.L. 1996. The size distribution of framboidal pyrite in modern sediments: an indicator of redox conditions. Geochimica et Cosmochimica Acta. 60:3897–3912.

Yurewicz, D. A., 1977. Sedimentology of Mississippian basin-facies carbonates, New Mexico and West Texas: Society of Economic Paleontologists and Mineralogists, no. 25 p.203 - 219.

Biographical Information

Chizoba Charity Nsianya graduated with a B.S and Post graduate diploma in geology from Nnamdi Azikiwe University and University of Port Harcourt Nigeria respectively. She moved to the United States in 2006 and was delighted to join the University of Texas at Arlington for her M.S. in 2011. She worked under the supervision of Dr. H. Rowe and studied shale geochemistry.